Max-Planck-Institut für Radioastronomie

Julius-Maximilians-UNIVERSITÄT WÜRZBURG

IMPRS astronomy & astrophysics Bonn and Cologne

Gamma-ray emission in radio galaxies under the VLBI scope

R. Angioni (MPIfR-Bonn, U. Würzburg)

Monitoring the non-thermal universe 2018, Cochem

Collaborators:
Prof. E. Ros (MPIfR-Bonn)
Prof. M. Kadler (U. Würzburg)
Dr. R. Ojha (NASA/GSFC/UMBC)
et al., for the TANAMI and *Fermi*-LAT collaborations

The radio-gamma connection in AGN

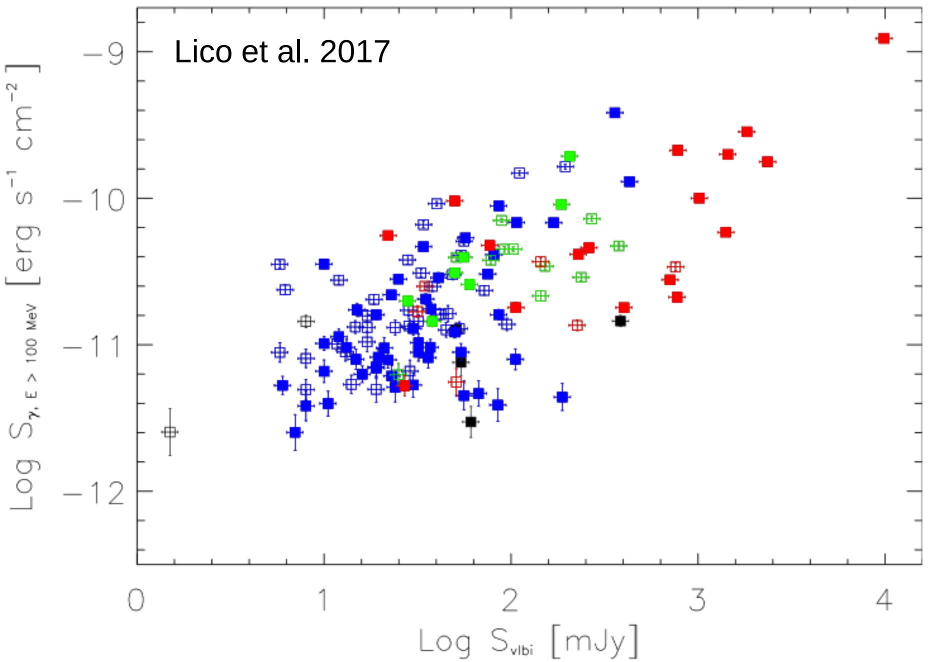

Strong connection between radio and γ-ray emission in large, blazar-dominated samples (e.g., Kovalev+09, Ackermann+11, Lico+17)

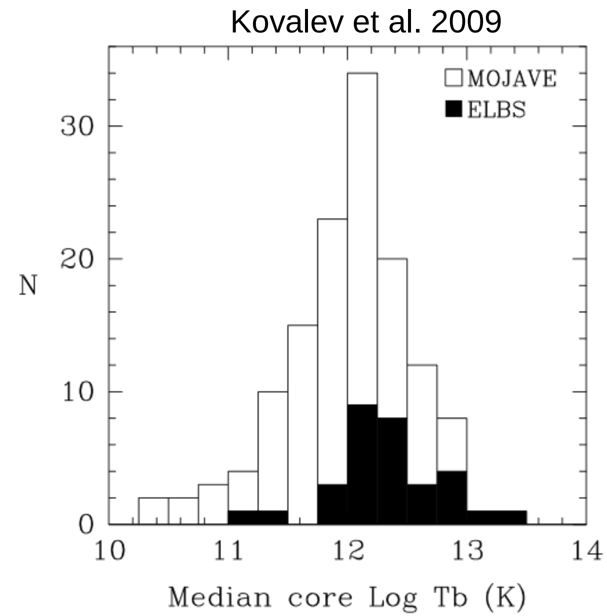

γ-ray sources in large radio samples show preferentially higher Doppler boosting markers (Kovalev+09)

Image credit: DESY science communications

Image credit: DESY science communications

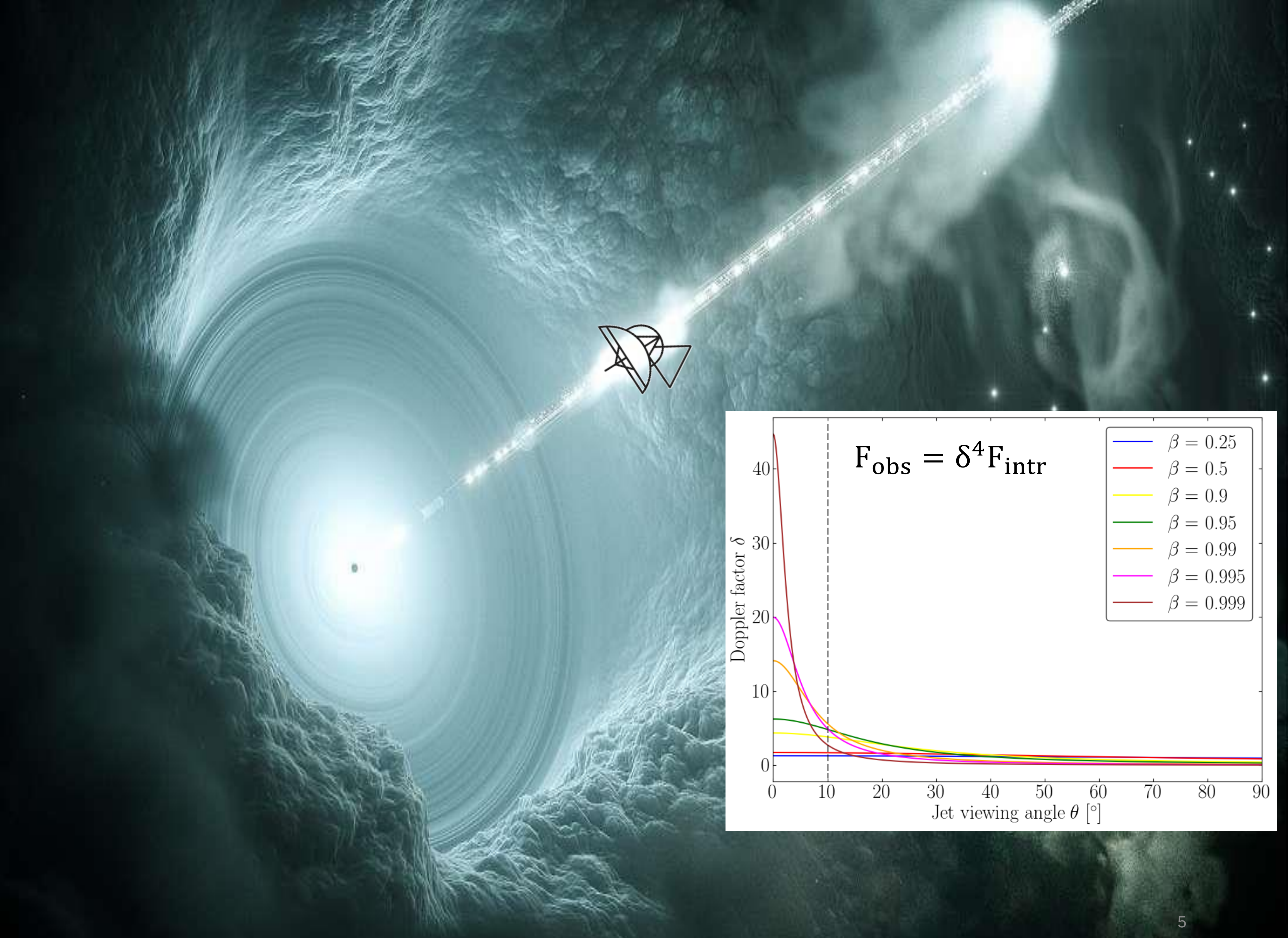

Image credit: DESY science communications

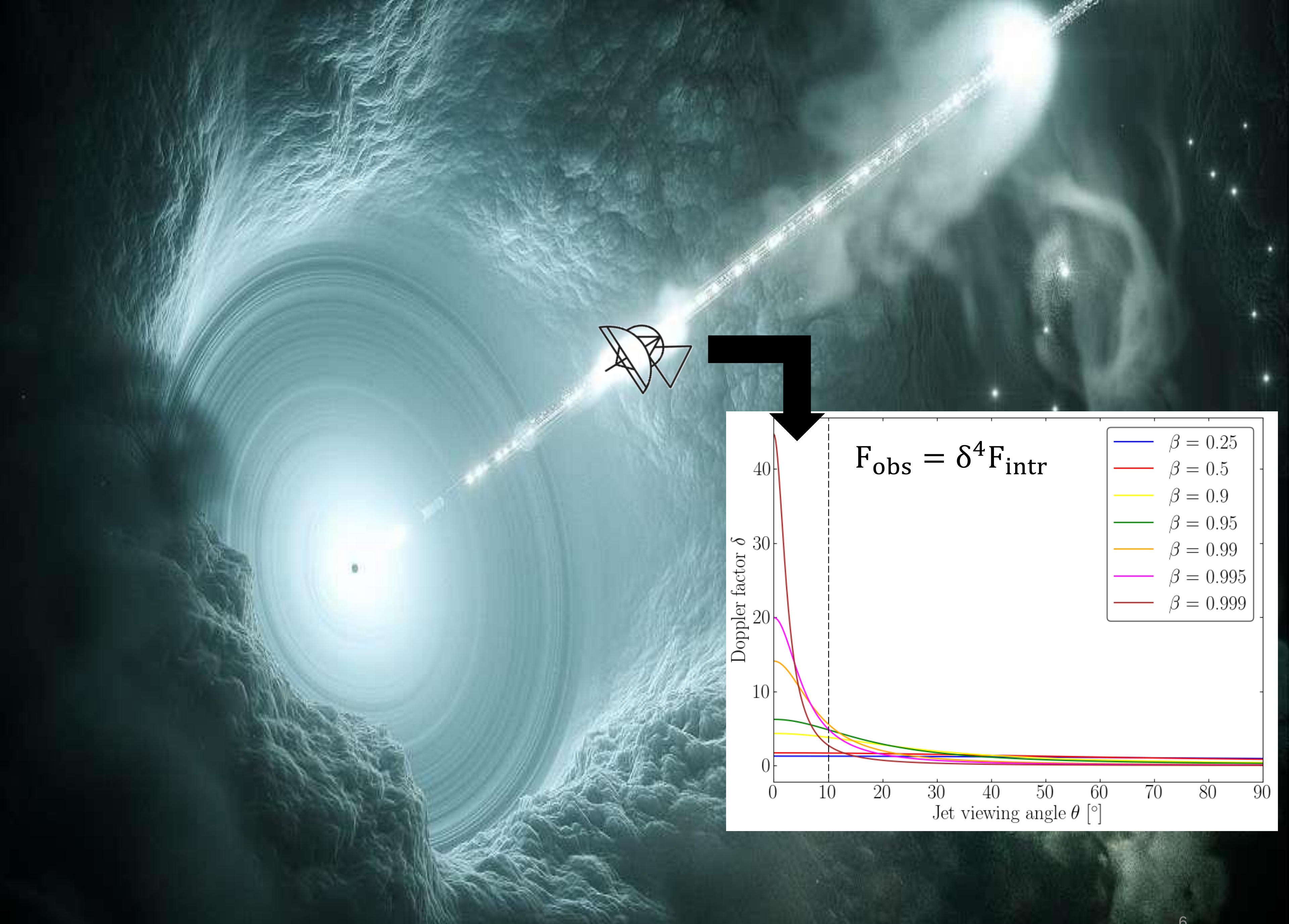

Image credit: DESY science communications

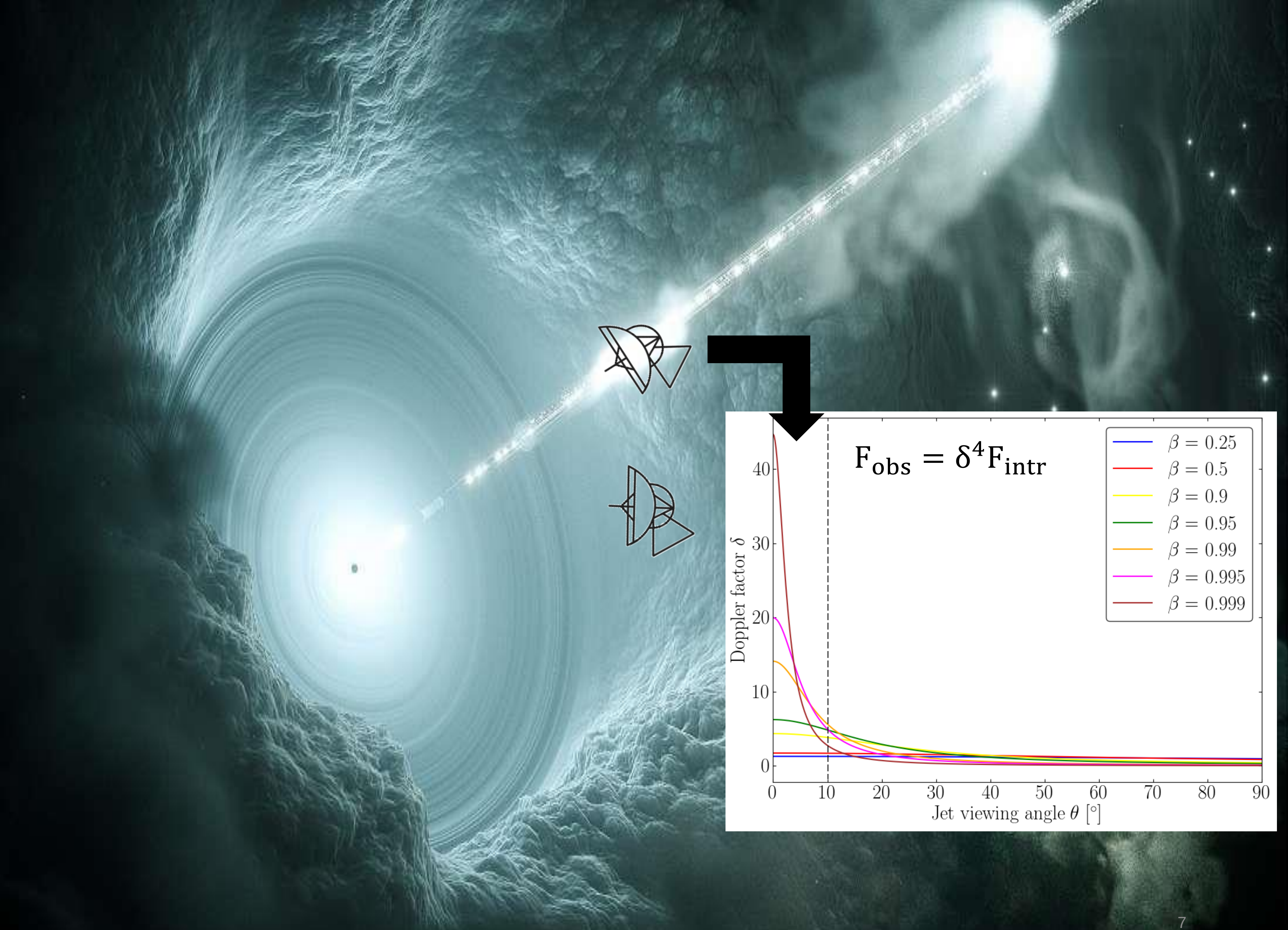

Image credit: DESY science communications

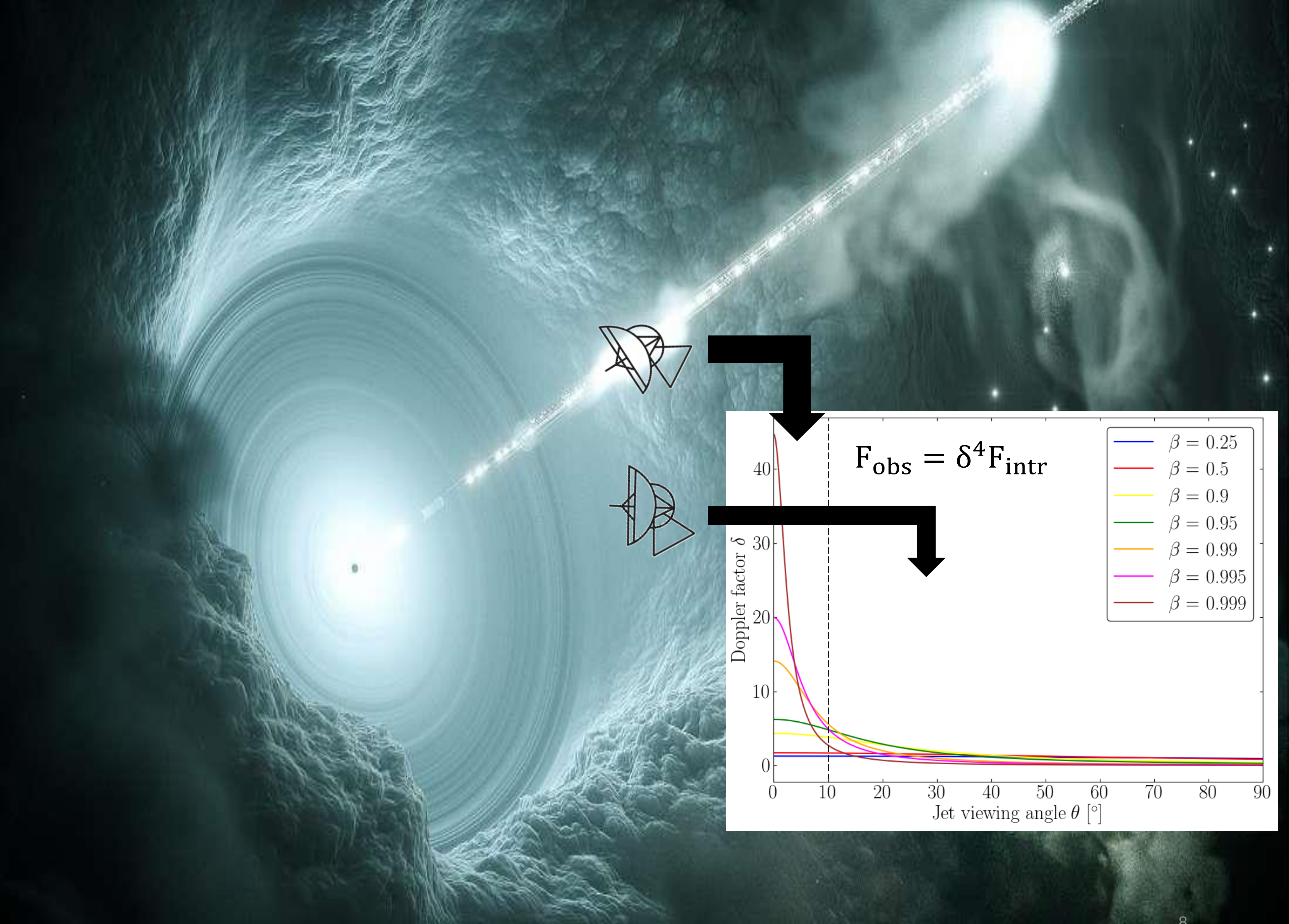

Image credit: DESY science communications

Radio and γ-ray properties of radio galaxies

- Well-established relationship between pc-scale jet and γ-rays in blazars

Radio and γ-ray properties of radio galaxies

- Well-established relationship between pc-scale jet and γ-rays in blazars
- Much less clear situation for radio galaxies
  - Mostly single-source studies (e.g. 3C 111, 3C 120, M 87, NGC 1275)
  - No systematic population study of VLBI-LAT properties of radio galaxies

Radio and γ-ray properties of radio galaxies

- Well-established relationship between pc-scale jet and γ-rays in blazars
- Much less clear situation for radio galaxies
  - Mostly single-source studies (e.g. 3C 111, 3C 120, M 87, NGC 1275)
  - No systematic population study of VLBI-LAT properties of radio galaxies

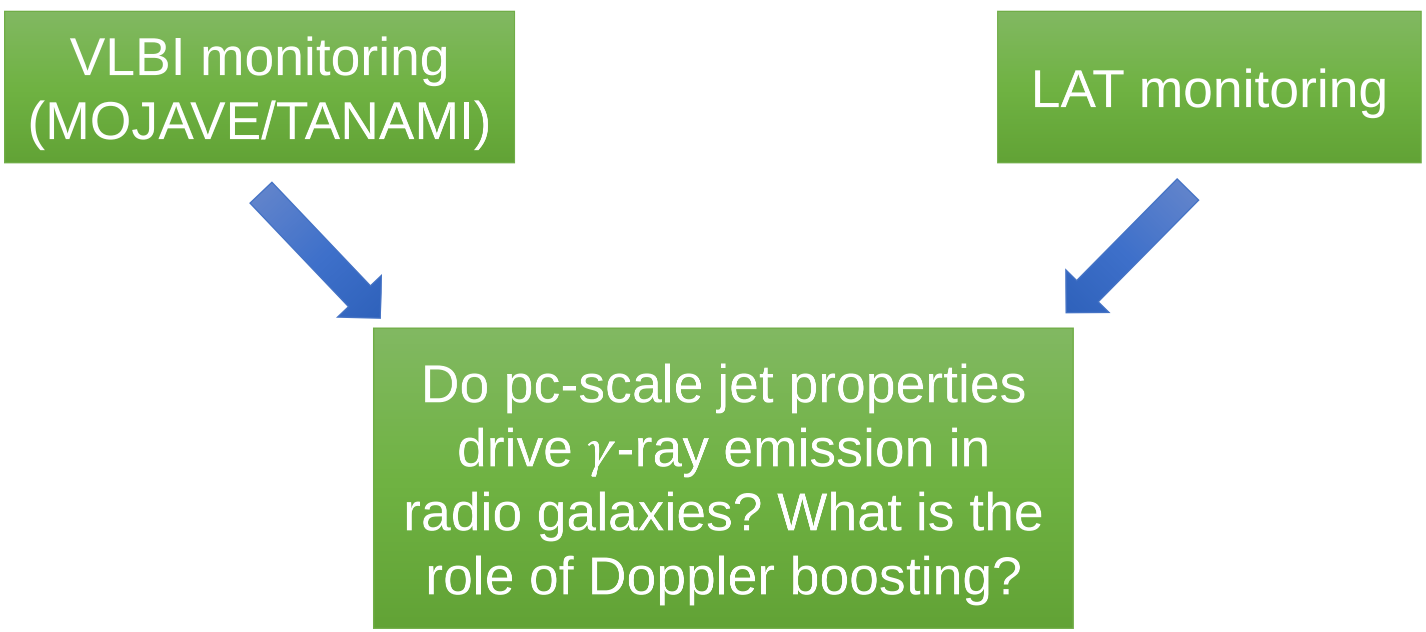

The TANAMI program

Tracking Active Nuclei with Austral Milliarcsecond Interferometry

- ~100 jets at $\delta < -30^{\circ}$ declination at mas resolution since 2007
- Dual frequency 8.4 GHz and 22.3 GHz, 3-4 epochs/yr

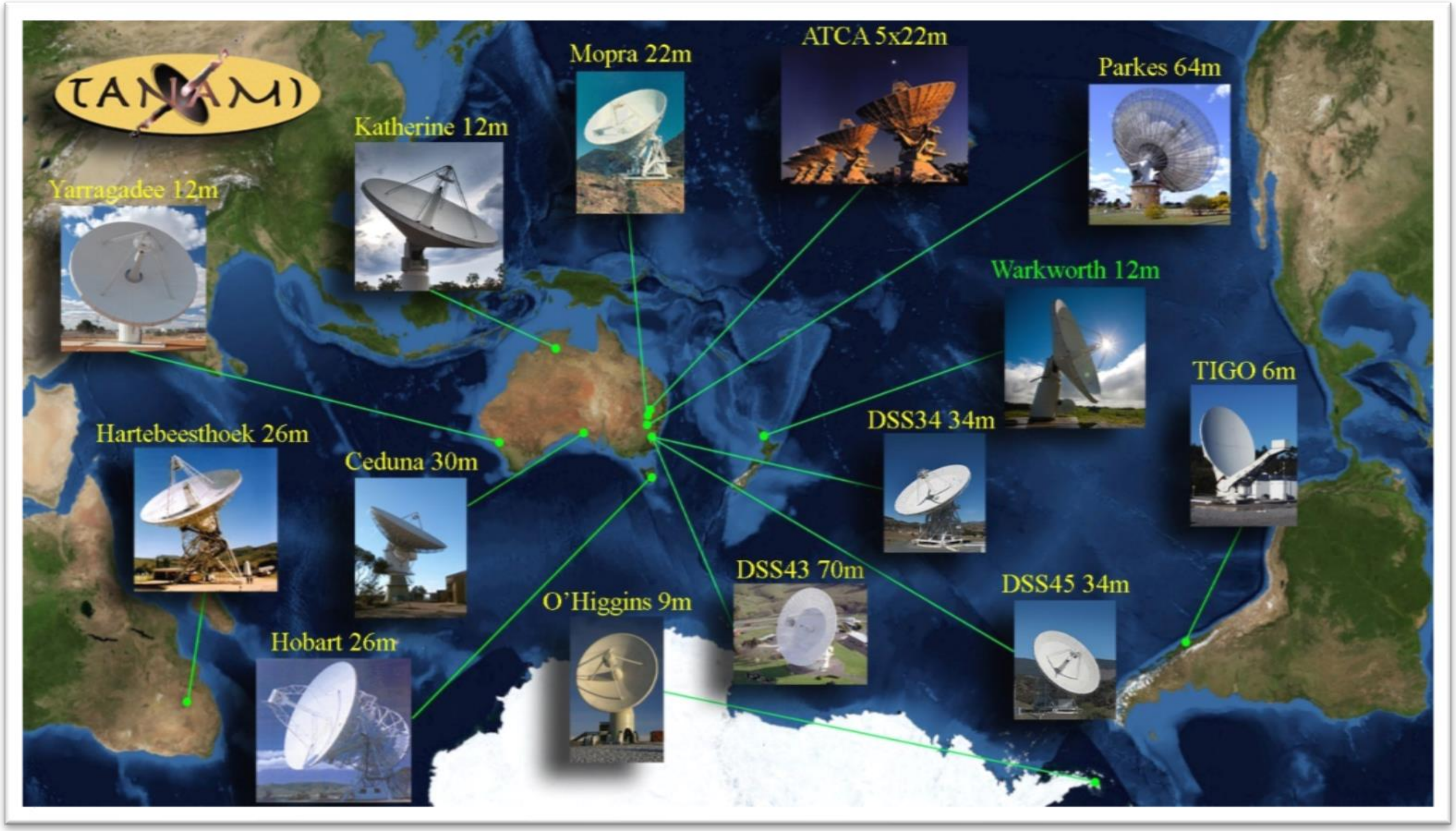

TANAMI radio galaxy sample

B1950 name	Catalog name	Class[a]	Redshift	RA(J2000)	Dec(J2000)	LAT[b]
0518−458	Pictor A	FR II	0.035	79.957	−45.779	yes
0521−365	PKS 0521−36	RG/SSRQ	0.057	80.742	−36.459	yes
0625−354	PKS 0625−35	FR I/BLL	0.055	96.778	−35.487	yes
0825−500	PKS 0823−500	RG	-	126.362	−50.178	no
1258−321	PKS 1258−321	FR I	0.017	195.253	−32.441	no
1322−428	Centaurus A	FR I	0.0018	201.365	−43.019	yes
1333−337	IC 4296	FR I	0.013	204.162	−33.966	no
1343−601	Centaurus B	FR I	0.013	206.704	−60.408	yes
1549−790	PKS 1549−79	RG/CFS	0.15	239.245	−79.234	no
1600−489	PMN J1603−4904	MSO[c]	0.23[d]	240.961	−49.068	yes
1718−649	PKS 1718−649	GPS/CSO	0.014	260.921	−65.010	yes[e]
1733−565	PKS 1733−56	FR II	0.098	264.399	−56.567	no
1814−637	PKS 1814−63	CSS/CSO	0.065	274.896	−63.763	no
2027−308	PKS 2027−308	RG	0.54	307.741	−30.657	no
2152−699	PKS 2153−69	FR II	0.028	329.275	−69.690	no

TANAMI radio galaxy sample

B1950 name	Catalog name	Class[a]	Redshift	RA(J2000)	Dec(J2000)	LAT[b]
0518−458	Pictor A	FR II	0.035	79.957	−45.779	yes
0521−365	PKS 0521−36	RG/SSRQ	0.057	80.742	−36.459	yes
0625−354	PKS 0625−35	FR I/BLL	0.055	96.778	−35.487	yes
0825−500	PKS 0823−500	RG	-	126.362	−50.178	no
1258−321	PKS 1258−321	FR I	0.017	195.253	−32.441	no
1322−428	Centaurus A	FR I	0.0018	201.365	−43.019	yes
1333−337	IC 4296	FR I	0.013	204.162	−33.966	no
1343−601	Centaurus B	FR I	0.013	206.704	−60.408	yes
1549−790	PKS 1549−79	RG/CFS	0.15	239.245	−79.234	no
1600−489	PMN J1603−4904	MSO[c]	0.23[d]	240.961	−49.068	yes
1718−649	PKS 1718−649	GPS/CSO	0.014	260.921	−65.010	yes[e]
1733−565	PKS 1733−56	FR II	0.098	264.399	−56.567	no
1814−637	PKS 1814−63	CSS/CSO	0.065	274.896	−63.763	no
2027−308	PKS 2027−308	RG	0.54	307.741	−30.657	no
2152−699	PKS 2153−69	FR II	0.028	329.275	−69.690	no

Pictor A

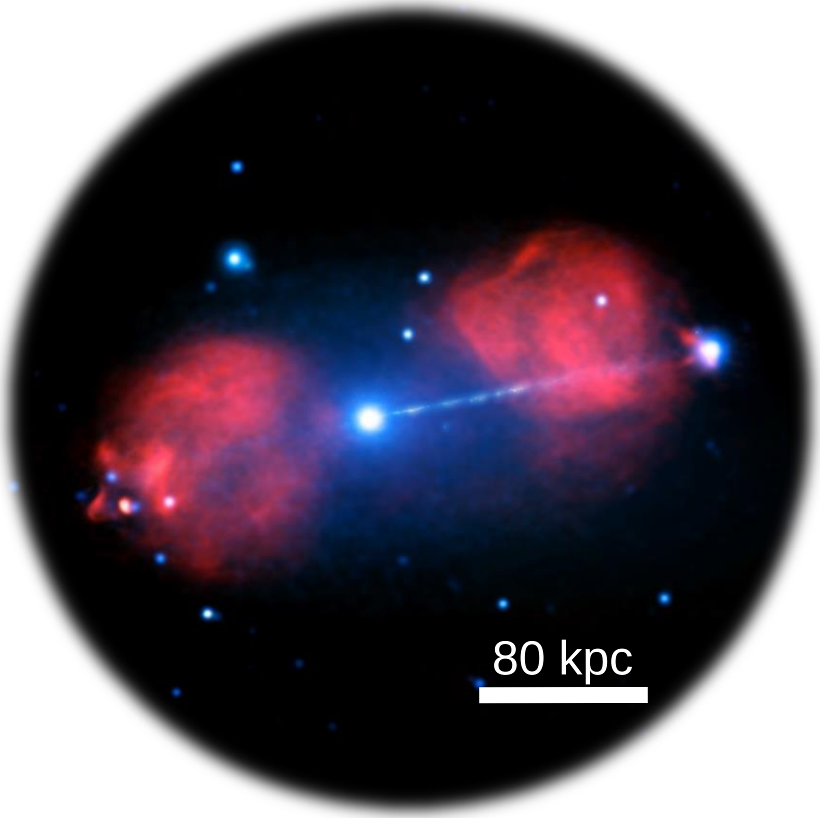

Image credit:
X-ray: NASA/CXC/Univ. of Hertfordshire/M. Hardcastle et al.
Radio: CSIRO/ATNF/ATCA

Classic FR II, $z = 0.035$

- Earlier VLBI study found jet viewing angle $\theta < 51°$ (Tingay+00)
- Detected by *Fermi*-LAT in 2012 (Brown+12) flux underestimated by SED model of western hot-spot, probably jet origin/contribution

Kinematic analysis: Pictor A

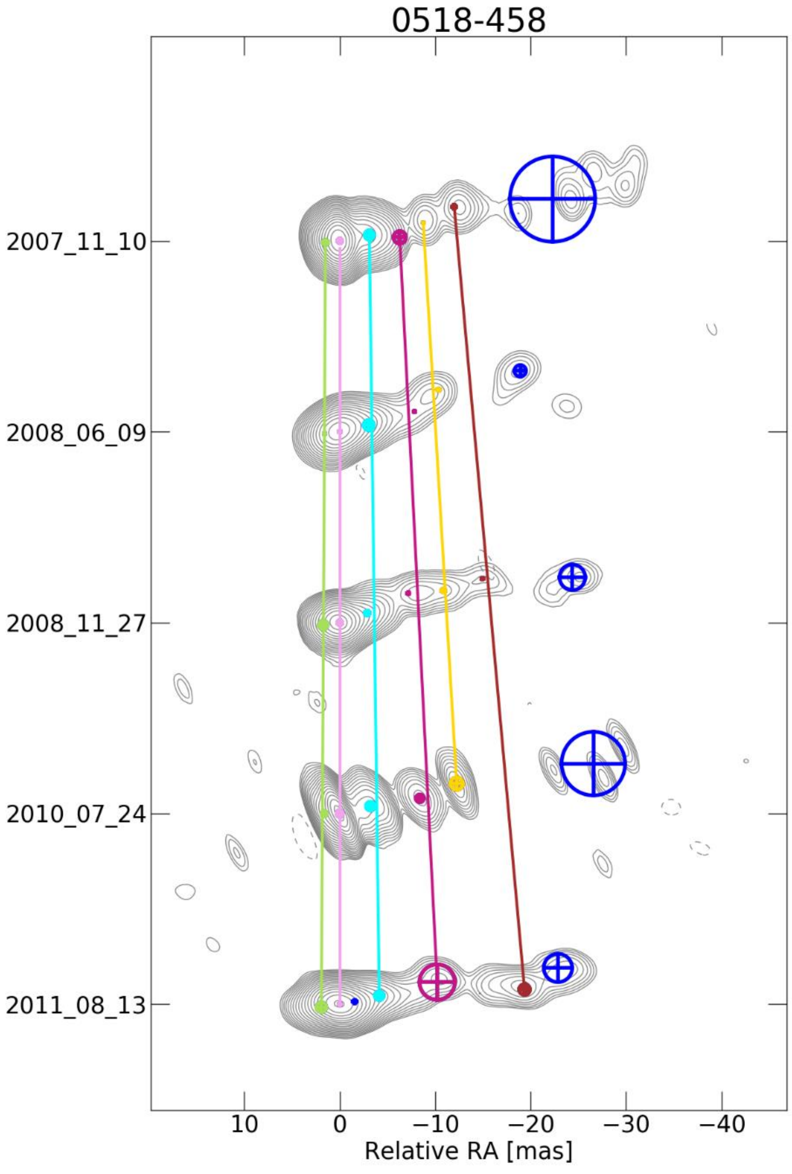

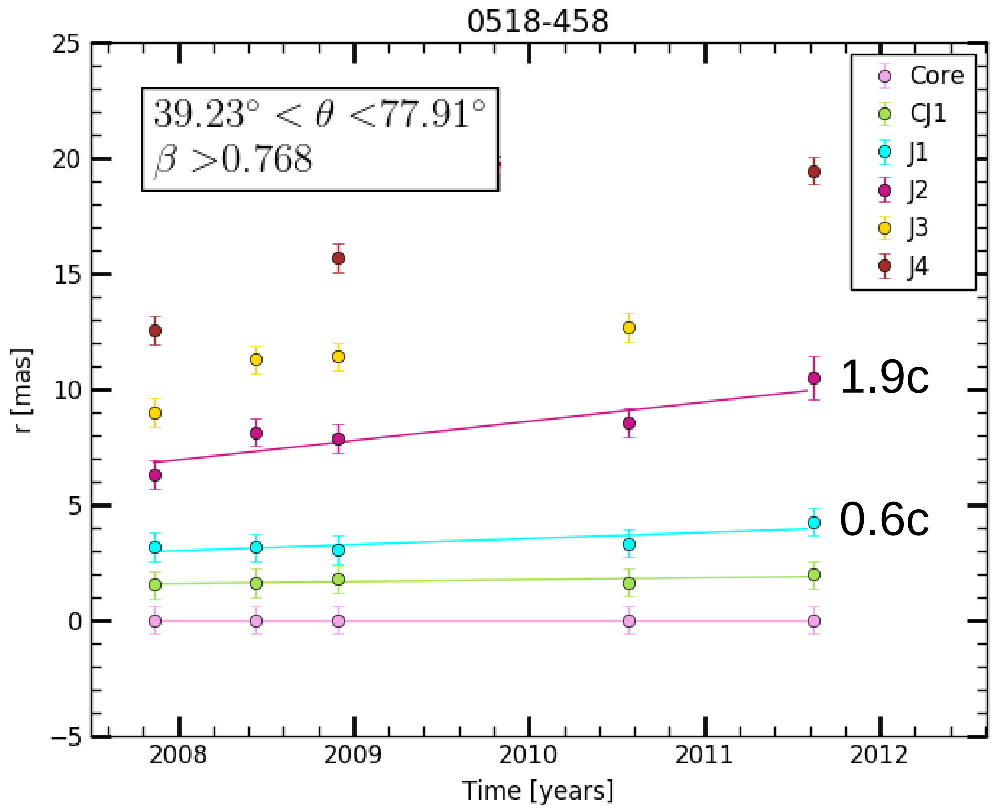

Angioni+ in prep.

Pictor A: jet emission confirmed?

LAT monthly light curve

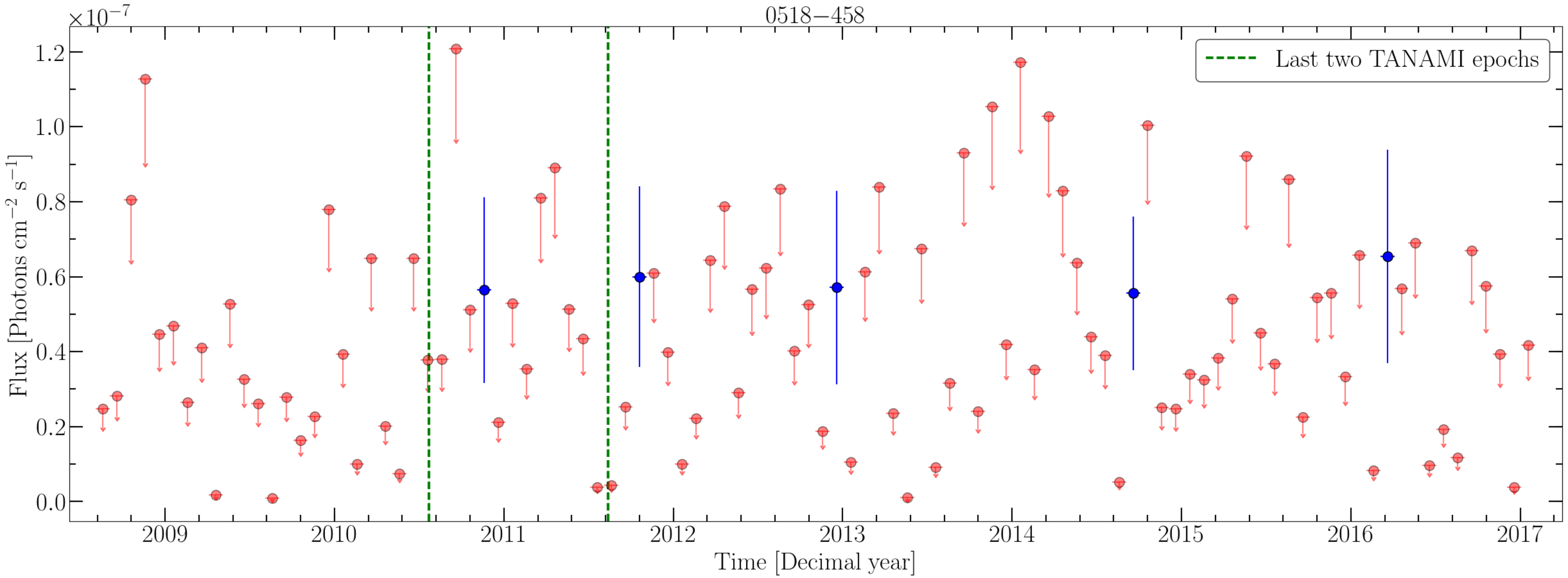

Angioni+ in prep.

Pictor A: jet emission confirmed?

LAT monthly light curve

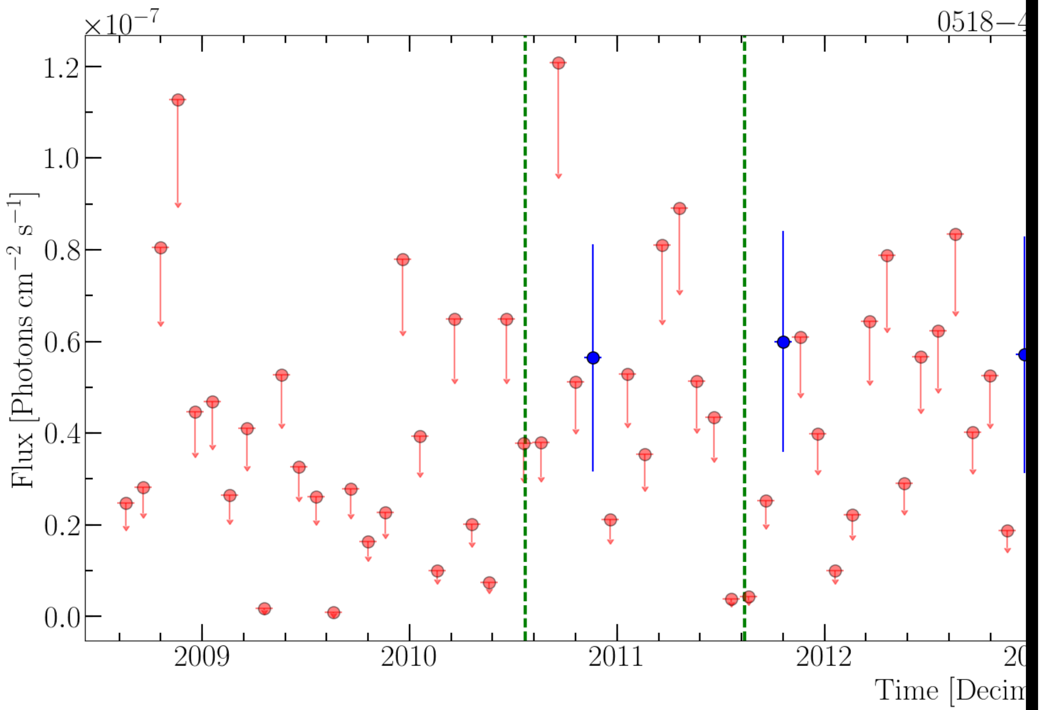

Angioni+ in prep.

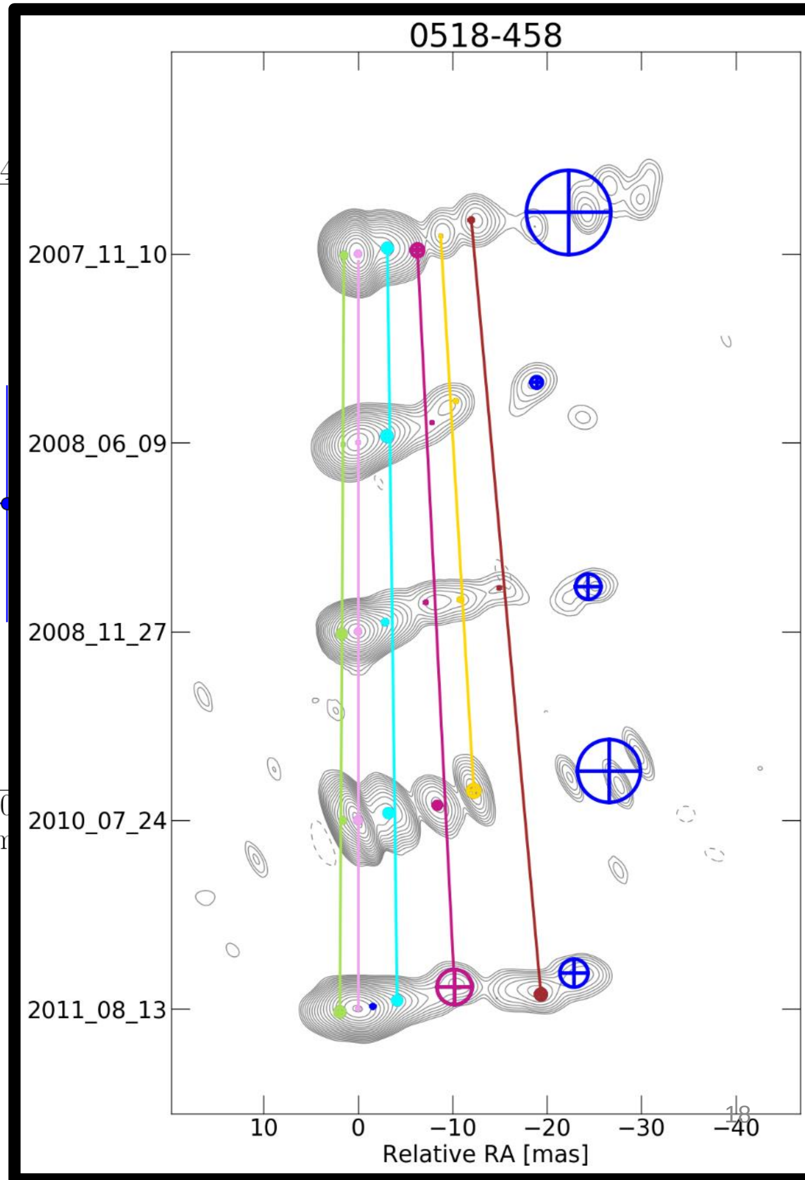

Pictor A: jet emission confirmed?

LAT monthly light curve

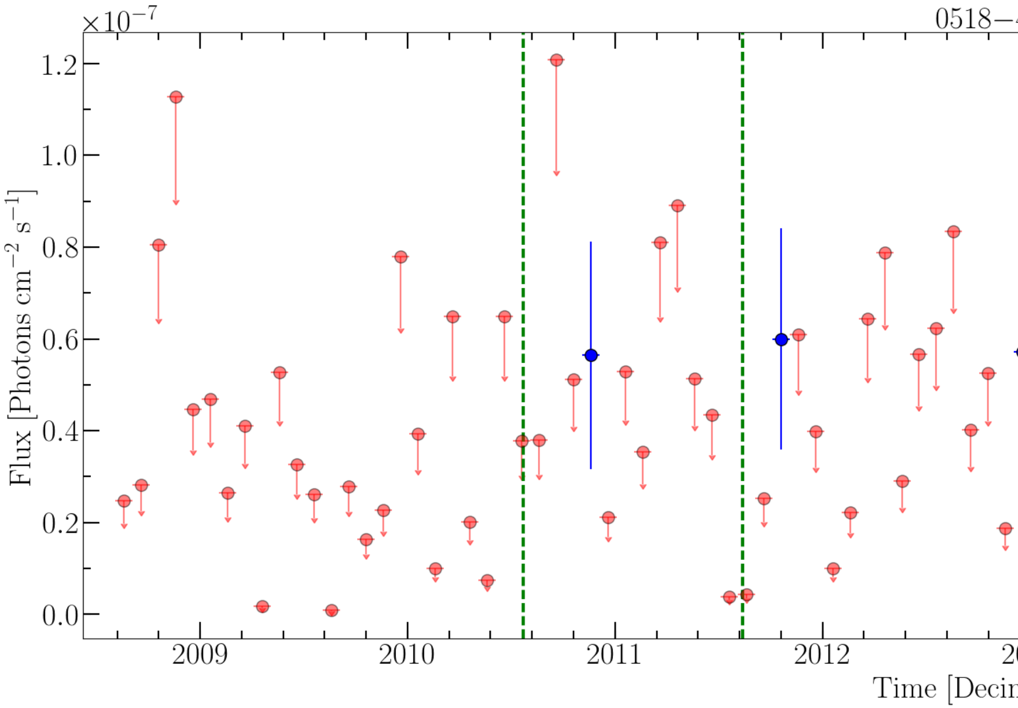

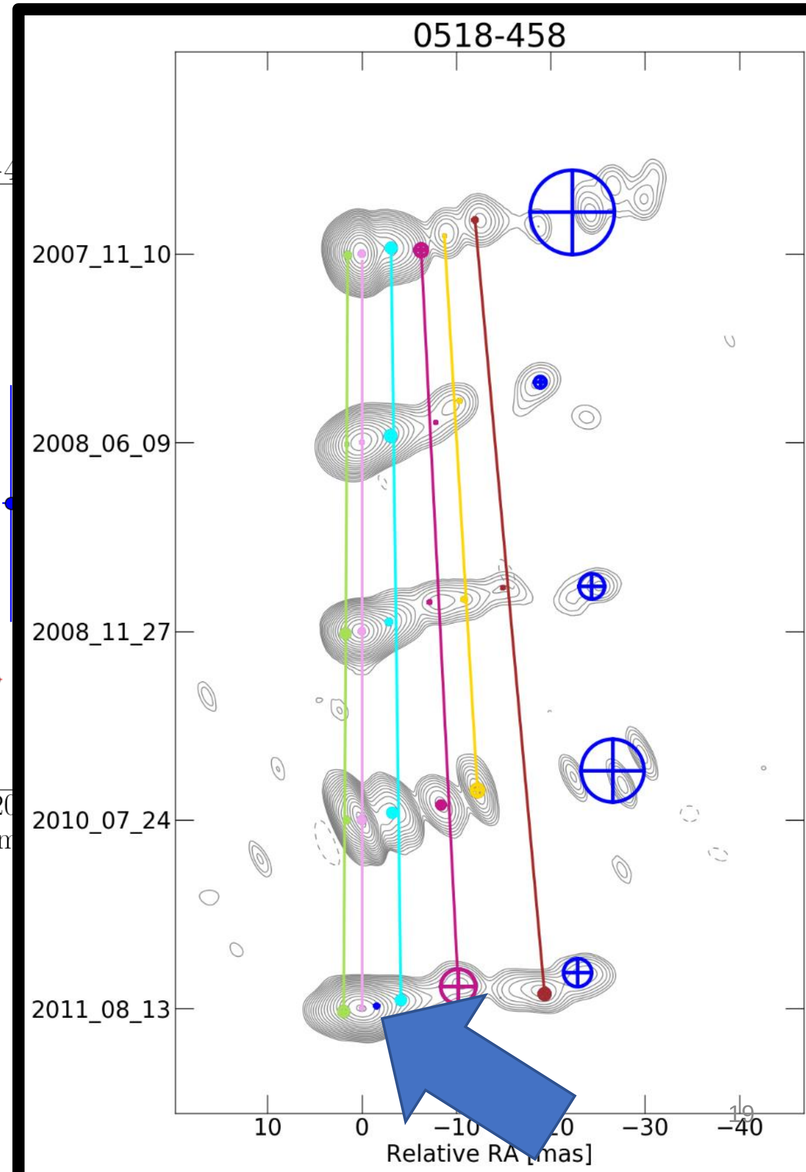

Angioni+ in prep.

PKS 0521–36

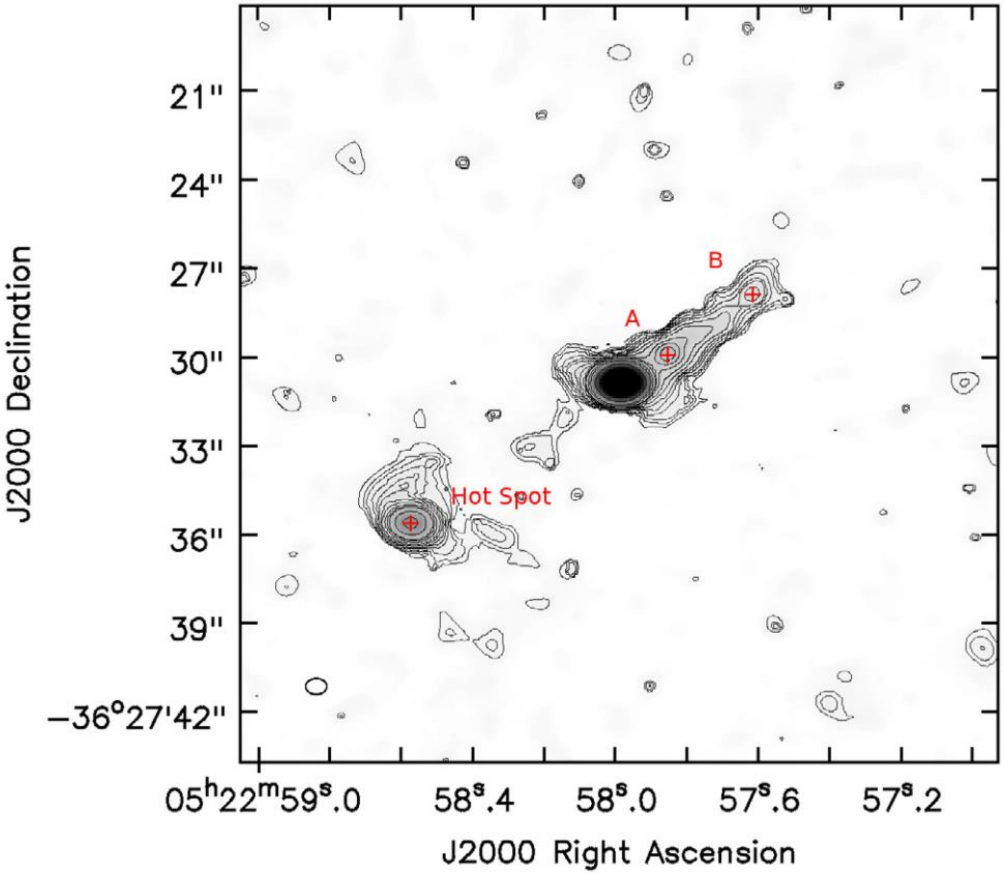

Misclassified BL Lac,
likely misaligned jet, $z = 0.055$

- Small core dominance suggests weak boosting (Pian+96)
- SED spine-sheath model suggests viewing angles $6° < \theta < 15°$ (D'Ammando+15)
- ALMA view of large-scale structure supports small beaming and large angle (Leon+16)

Image credit:
ALMA Bands 3,6,7 ($\nu_{\mathrm{eff}} \sim 220$ GHz): Leon et al. 2016

Kinematic analysis: PKS 0521−36

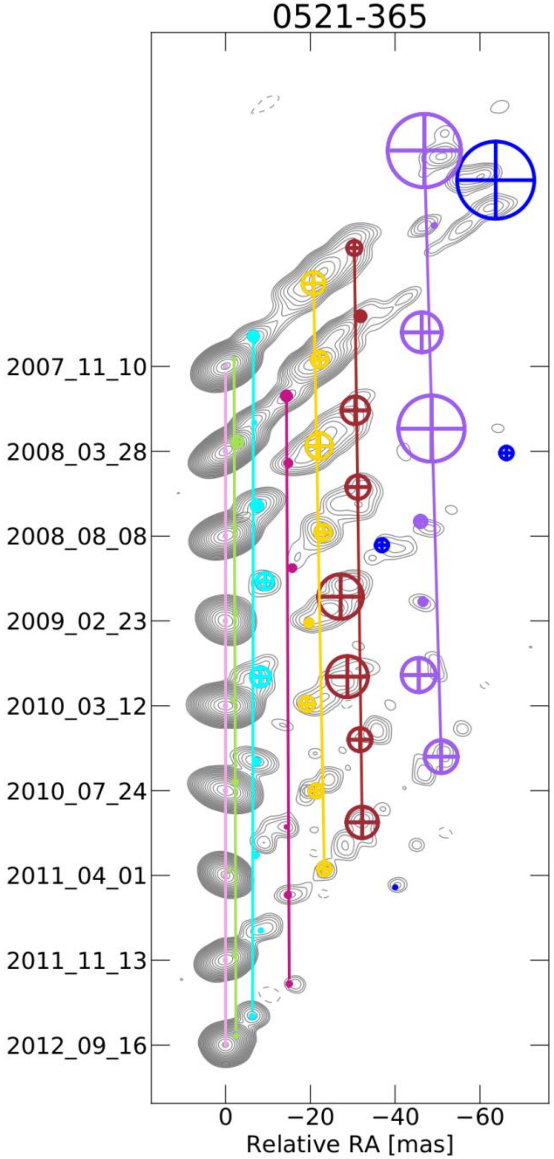

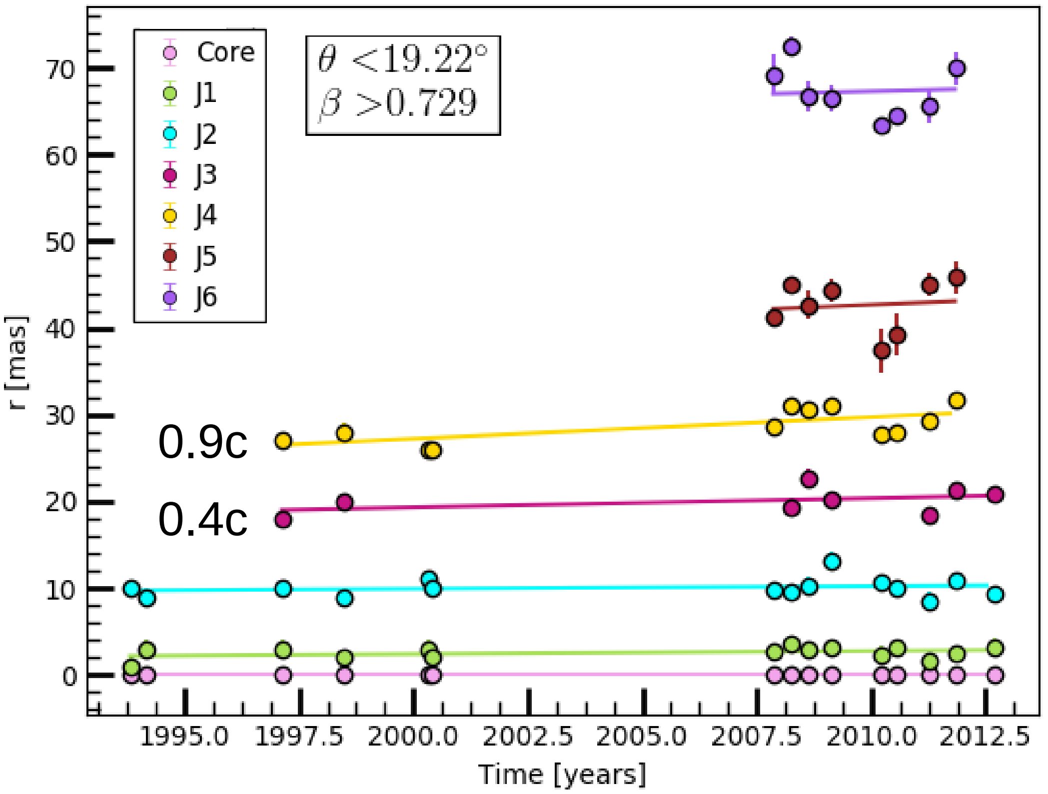

Angioni+ in prep.

PKS 0521−36: fast flares, slow jet

LAT weekly light curve

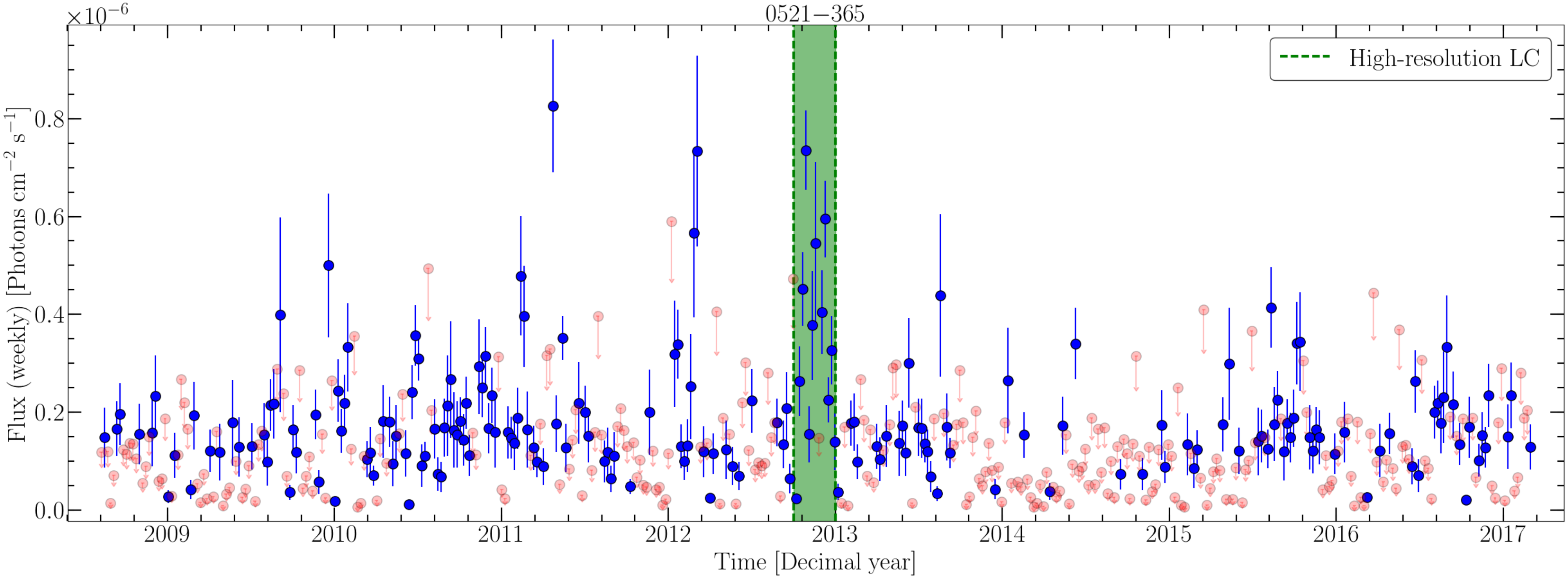

Angioni+ in prep.

PKS 0521−36: fast flares, slow jet

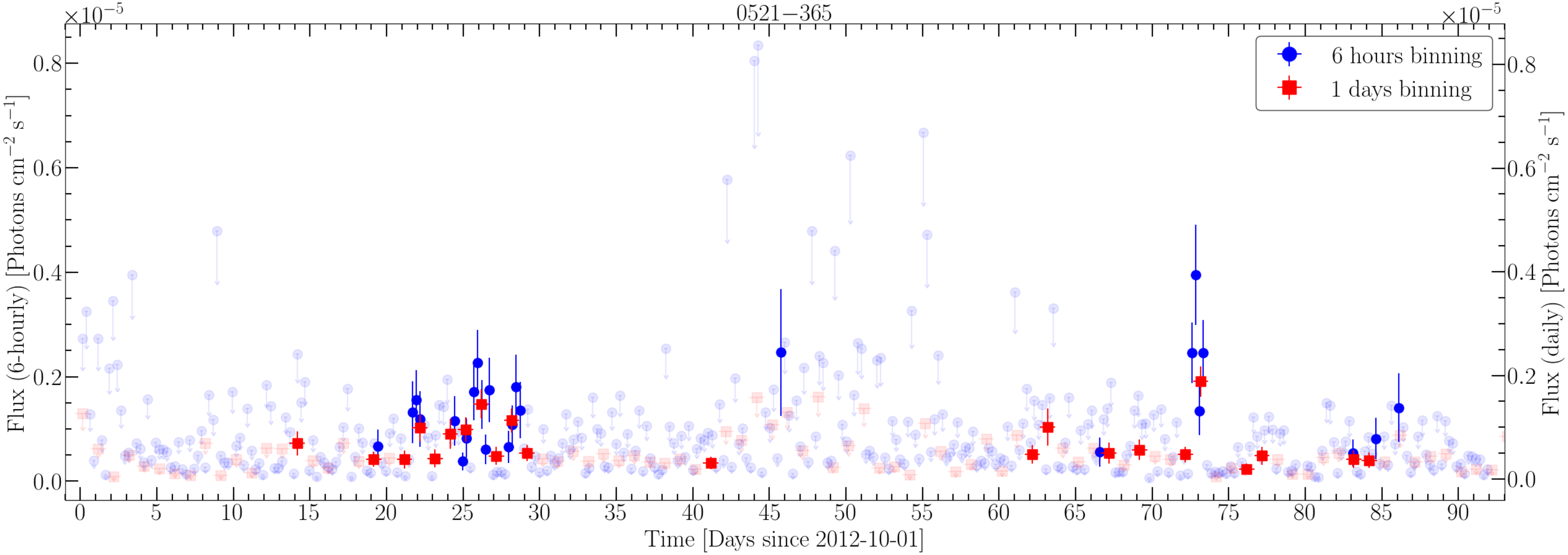

Angioni+ in prep.

TANAMI radio galaxy sample

B1950 name	Catalog name	Class[a]	Redshift	RA(J2000)	Dec(J2000)	LAT[b]
0518−458	Pictor A	FR II	0.035	79.957	−45.779	yes
0521−365	PKS 0521−36	RG/SSRQ	0.057	80.742	−36.459	yes
0625−354	PKS 0625−35	FR I/BLL	0.055	96.778	−35.487	yes
0825−500	PKS 0823−500	RG	-	126.362	−50.178	no
1258−321	PKS 1258−321	FR I	0.017	195.253	−32.441	no
1322−428	Centaurus A	FR I	0.0018	201.365	−43.019	yes
1333−337	IC 4296	FR I	0.013	204.162	−33.966	no
1343−601	Centaurus B	FR I	0.013	206.704	−60.408	yes
1549−790	PKS 1549−79	RG/CFS	0.15	239.245	−79.234	no
1600−489	PMN J1603−4904	MSO[c]	0.23[d]	240.961	−49.068	yes
1718−649	PKS 1718−649	GPS/CSO	0.014	260.921	−65.010	yes[e]
1733−565	PKS 1733−56	FR II	0.098	264.399	−56.567	no
1814−637	PKS 1814−63	CSS/CSO	0.065	274.896	−63.763	no
2027−308	PKS 2027−308	RG	0.54	307.741	−30.657	no
2152−699	PKS 2153−69	FR II	0.028	329.275	−69.690	no

Sample properties: extension to MOJAVE

Radio galaxies in the MOJAVE sample

B1950 name	Common name	Redshift	Flux[a]	Spectral index[b]	Curvature[c]	TS	Ref.[d]
0007+106	Mrk 1501	0.0893	$< 4 \times 10^{-9}$	-	-	1.87	[2]
0026+346	B2 0026+34	0.517	$< 3 \times 10^{-9}$	-	-	6.76	[2]
0055+300	*NGC 315*	0.0165	$(5.5 \pm 1.3) \times 10^{-9}$	2.29±0.11	-	77.3	[2]
0108+388	GB6 J0111+3906	0.668	$< 5 \times 10^{-9}$	-	-	2.95	[2]
0305+039	3C 78	0.0287	$(7.0 \pm 1.0) \times 10^{-9}$	1.96±0.07	-	385	[1]
0309+411	*NRAO 128*	0.136	$(5.7 \pm 1.7) \times 10^{-9}$	2.29±0.13	-	53.6	[2]
0316+413	3C 84	0.018	$(3.36 \pm 0.04) \times 10^{-7}$	2.006±0.008	0.060±0.004	9.63×10^{4}	[1]
0415+379	3C 111	0.0491	$(3.4 \pm 0.3) \times 10^{-8}$	2.75±0.07	-	186	[1]
0430+052	3C 120	0.033	$(2.8 \pm 0.3) \times 10^{-8}$	2.70±0.06	-	226	[1]
0710+439	B3 0710+439	0.518	$< 6 \times 10^{-10}$	-	-	0.0	[2]
1128−047	PKS 1128−047	0.27	$(7.6 \pm 1.3) \times 10^{-9}$	2.46±0.10	-	58.9	[2]
1228+126	M87	0.00436	$(1.9 \pm 0.2) \times 10^{-8}$	2.08±0.04	-	1410	[2]
1345+125	4C +12.50	0.121	$< 1 \times 10^{-9}$	-	-	0.97	[2]
1509+054	PMN J1511+0518	0.084	$< 2 \times 10^{-9}$	-	-	0.35	[2]
1514+004	*PKS 1514+00*	0.052	$(8.8 \pm 1.6) \times 10^{-9}$	2.46±0.10	-	82.3	[2]
1607+268	CTD 93	0.473	$< 7 \times 10^{-9}$	-	-	5.88	[2]
1637+826	NGC 6251	0.0247	$(2.2 \pm 0.2) \times 10^{-8}$	2.28±0.04	0.09±0.02	1610	[2]
1845+797	3C 390.3	0.0555	$< 2 \times 10^{-9}$	-	-	5.35	[2]
1957+405	Cygnus A	0.0561	$< 4 \times 10^{-9}$	-	-	2.76	[2]
2021+614	OW 637	0.227	$< 1 \times 10^{-8}$	-	-	18.6	[2]
2128+048	PKS 2127+04	0.99	$< 2 \times 10^{-9}$	-	-	0.2	[2]

VLBI core flux

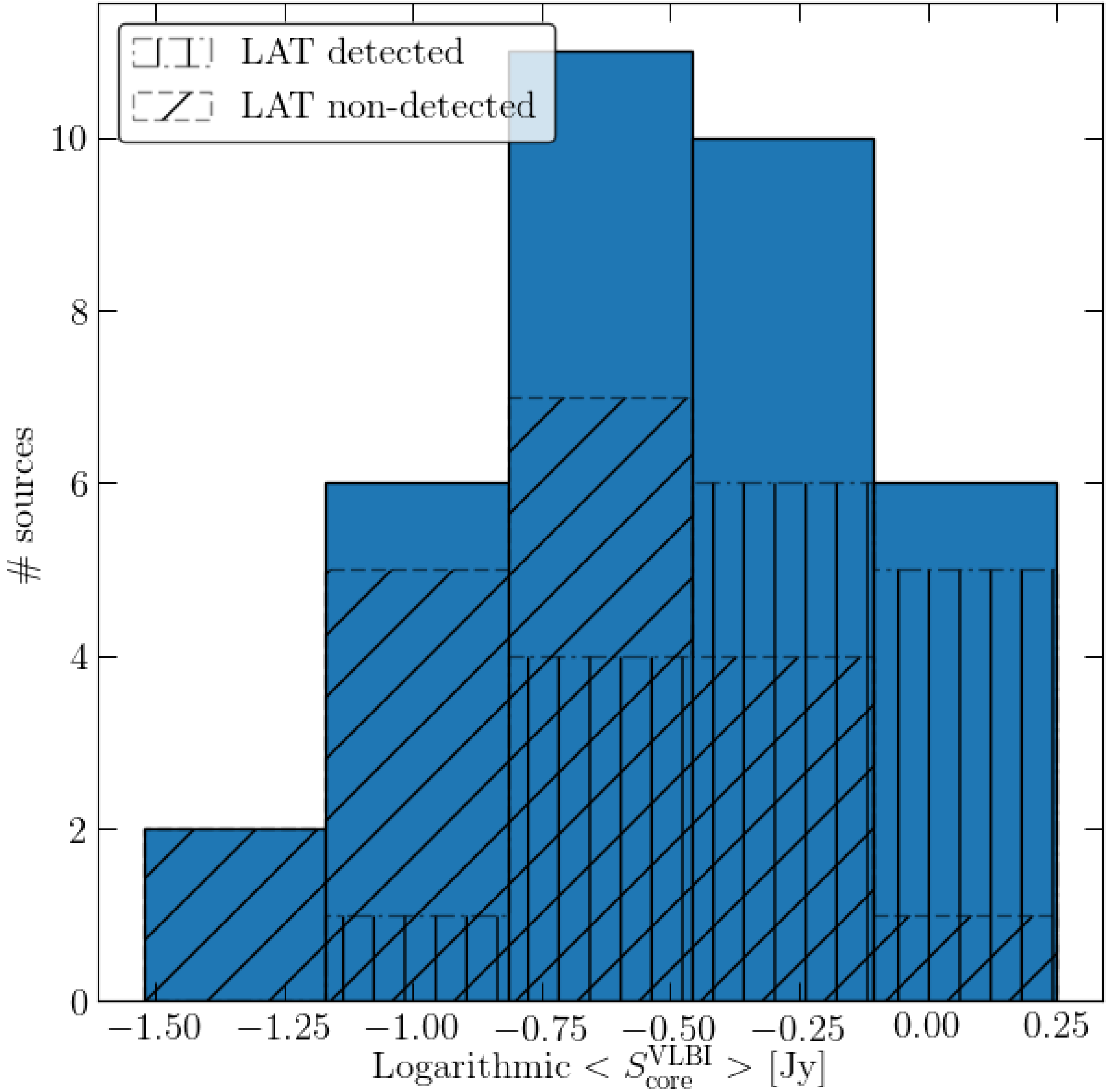

KS = 0.53
p-value = 0.009

VLBI core brightness temperature

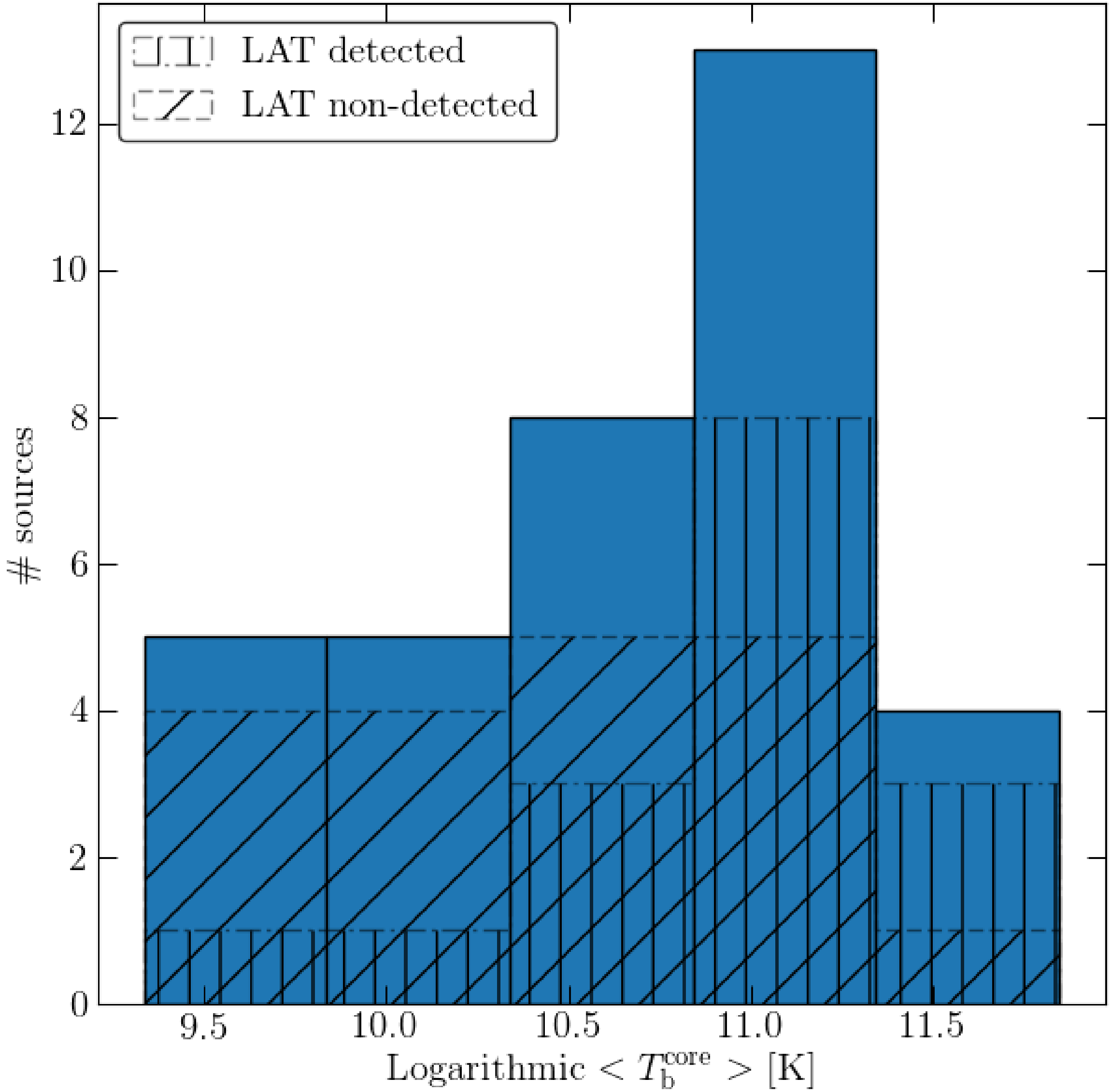

KS = 0.50
p-value = 0.017

$T_B \propto S/\theta^2$

VLBI core luminosity

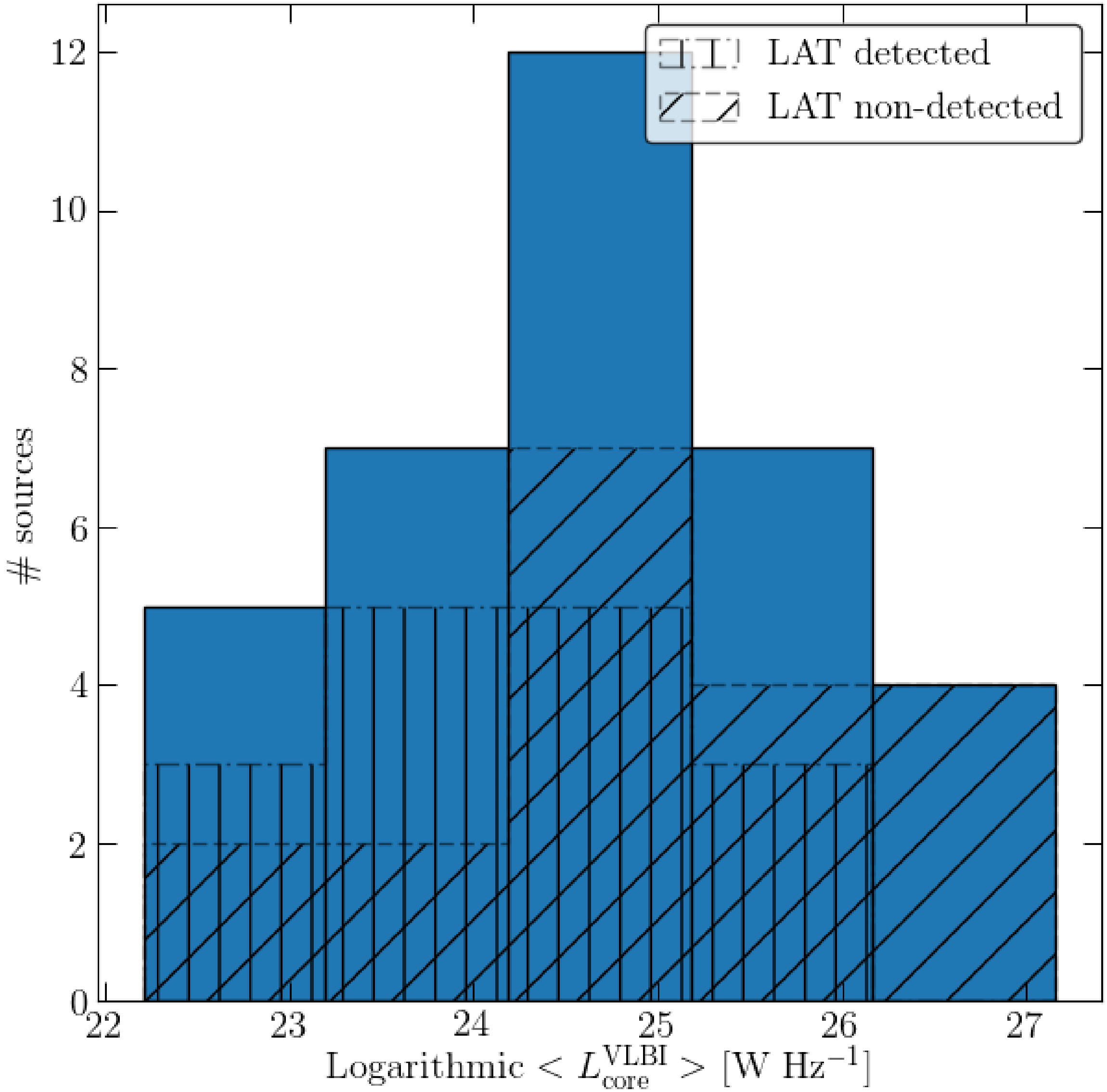

KS = 0.41
p-value = 0.073

VLBI jet flux

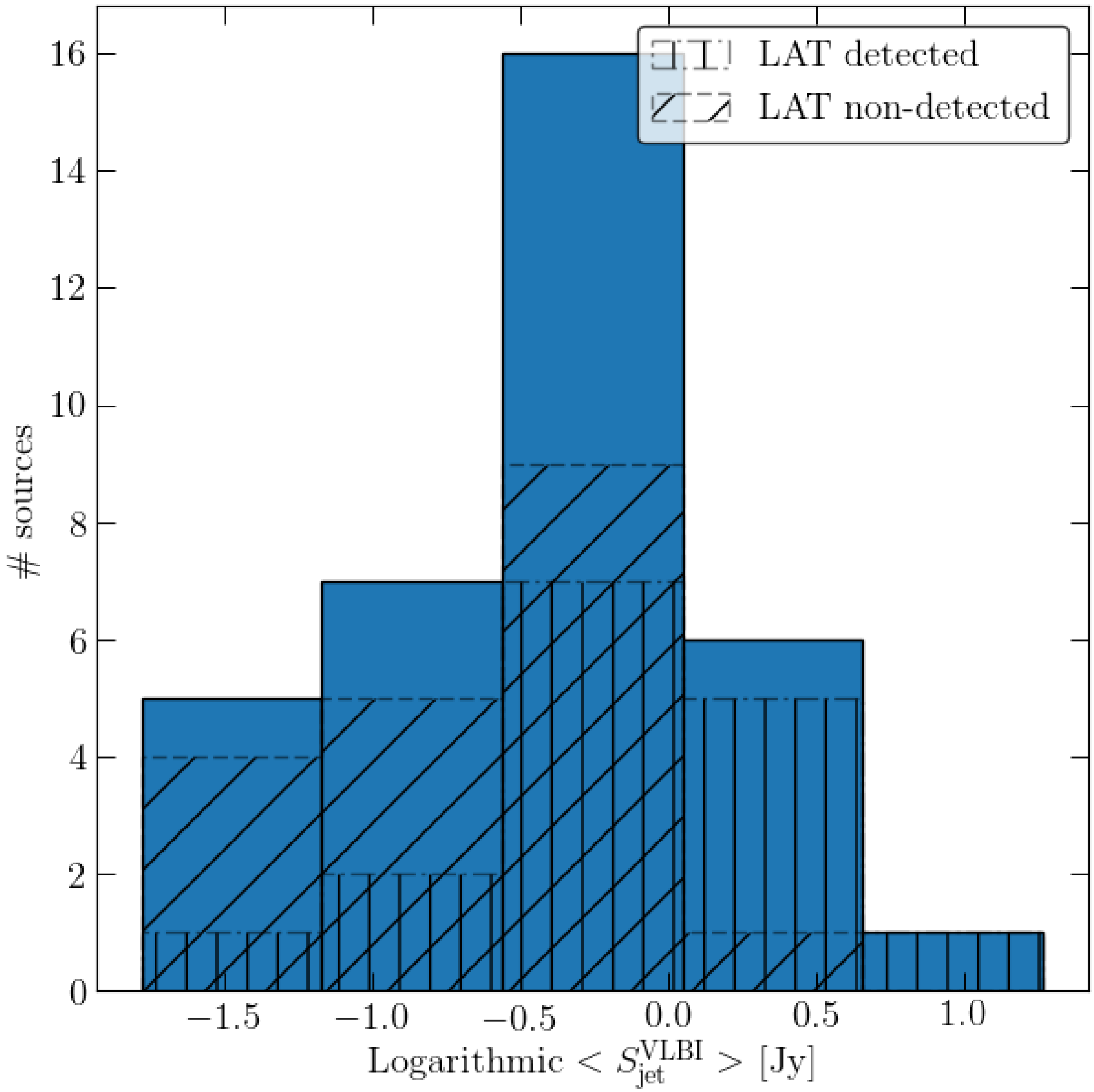

KS = 0.38
p-value = 0.13

$$S_{jet} = S_{tot} - S_{core}$$

Maximum apparent speed

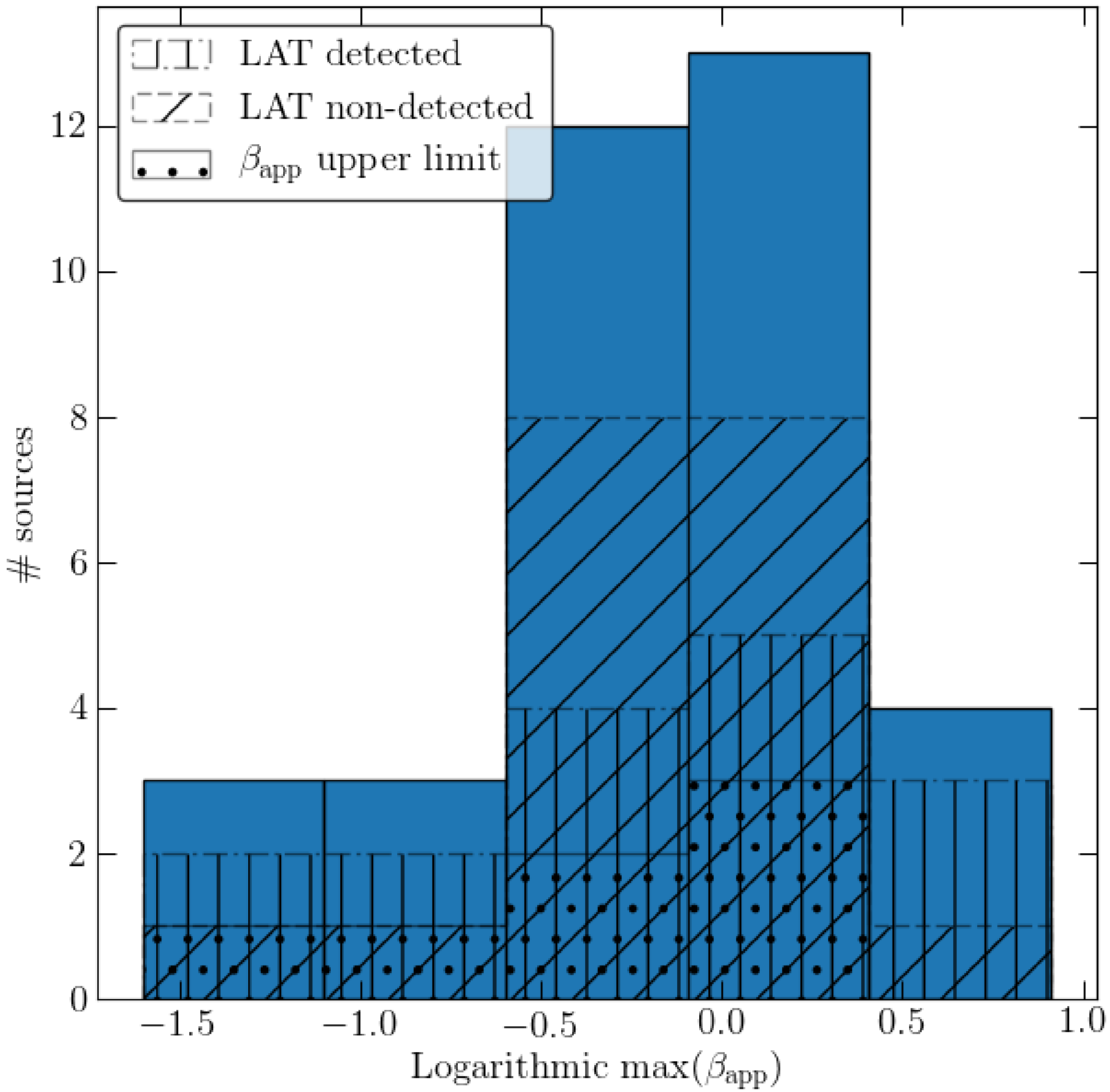

KS = 0.23
p-value = 0.70

VLBI core dominance

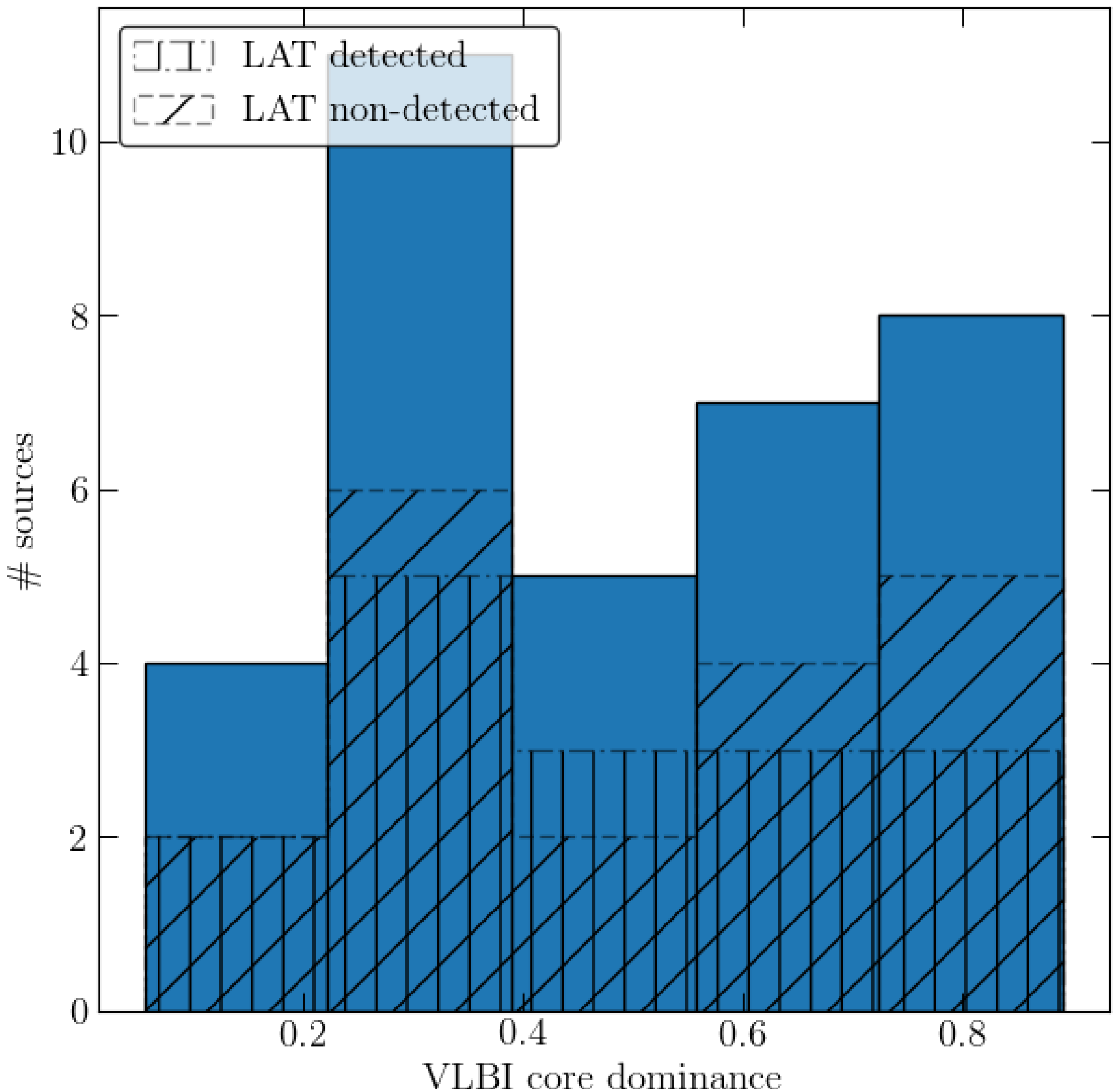

KS = 0.18
p-value = 0.91

$$CD = S_{core}/S_{tot}$$

LAT flux vs. VLBI core flux

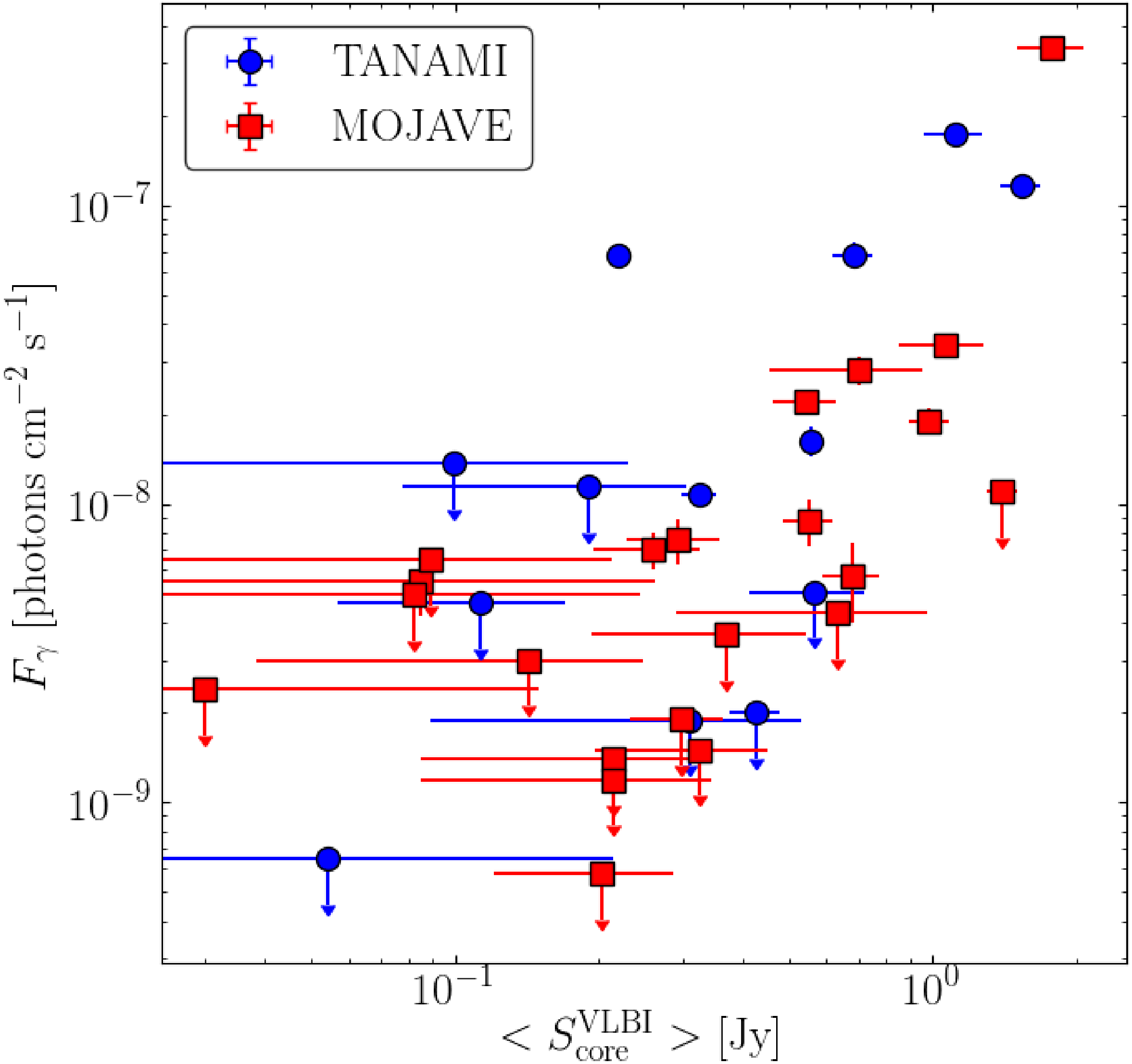

Kendall's tau
$\tau = 0.32$
p-value $= 0.006$

Compact radio emission is related to high-energy emission

LAT flux vs. VLBI jet flux

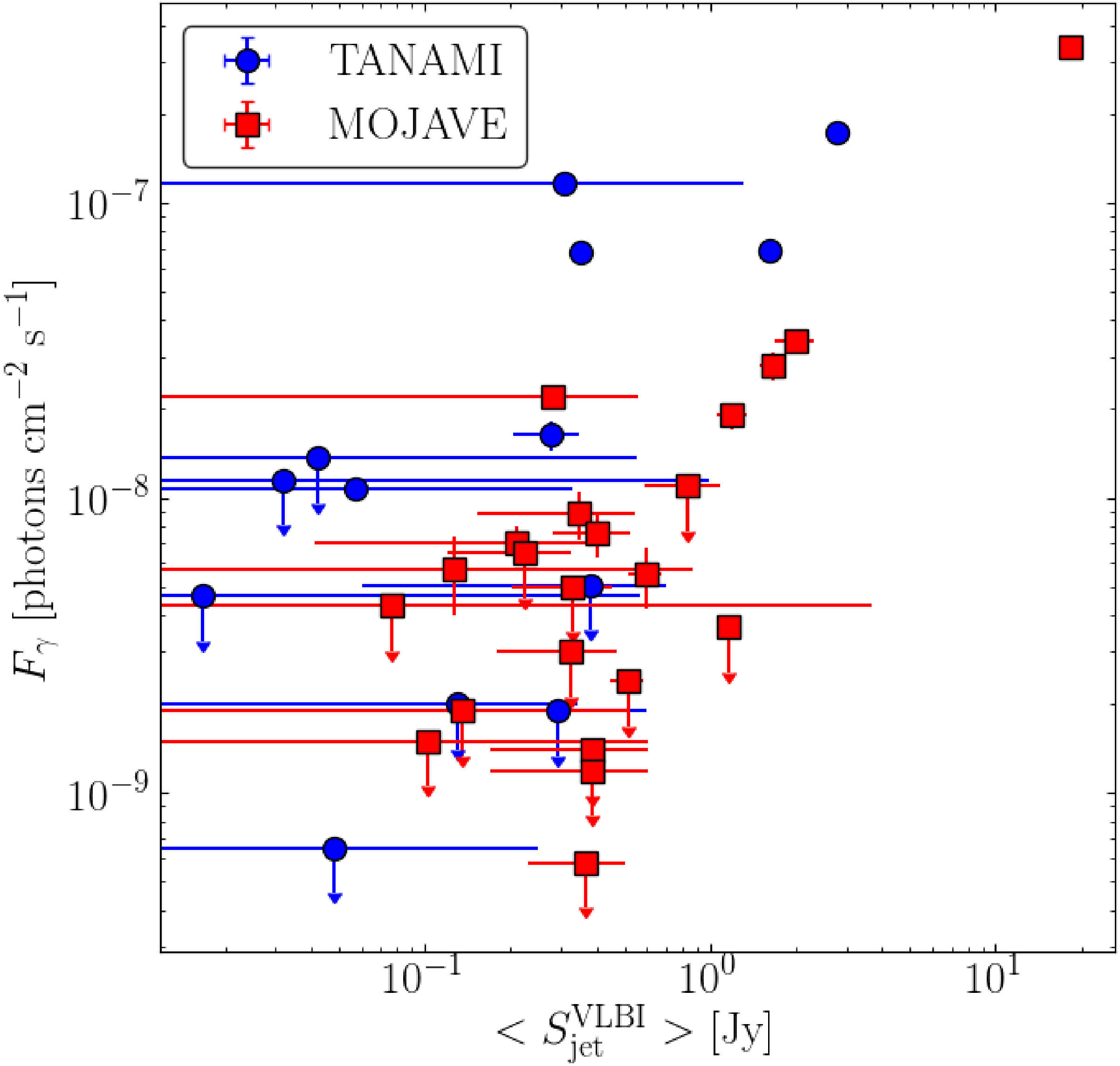

Kendall's tau

$\tau = 0.19$

p-value $= 0.1$

LAT luminosity vs. VLBI core luminosity

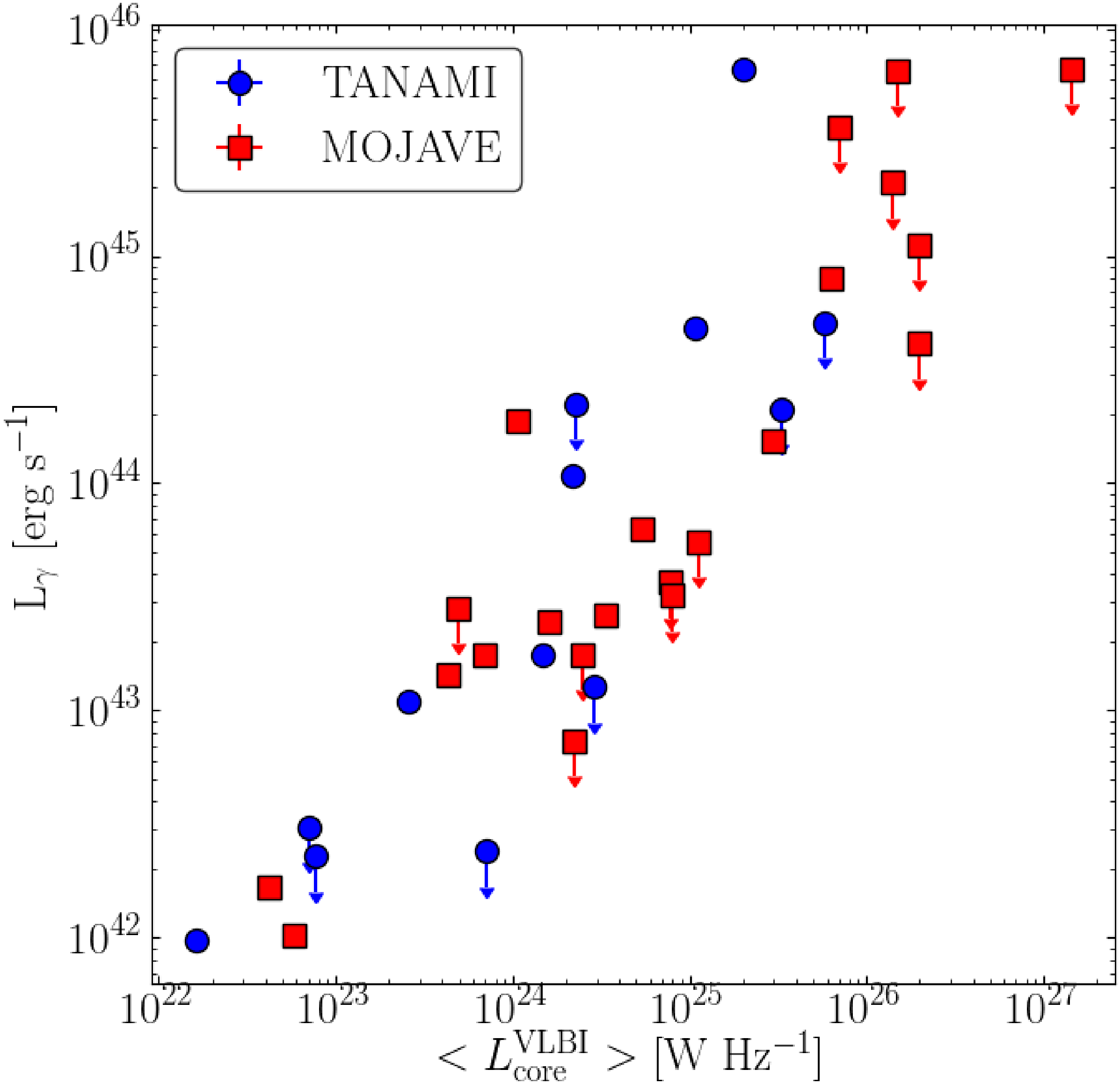

1:1 correlation induced by common redshift dependence

LAT luminosity vs. VLBI core dominance

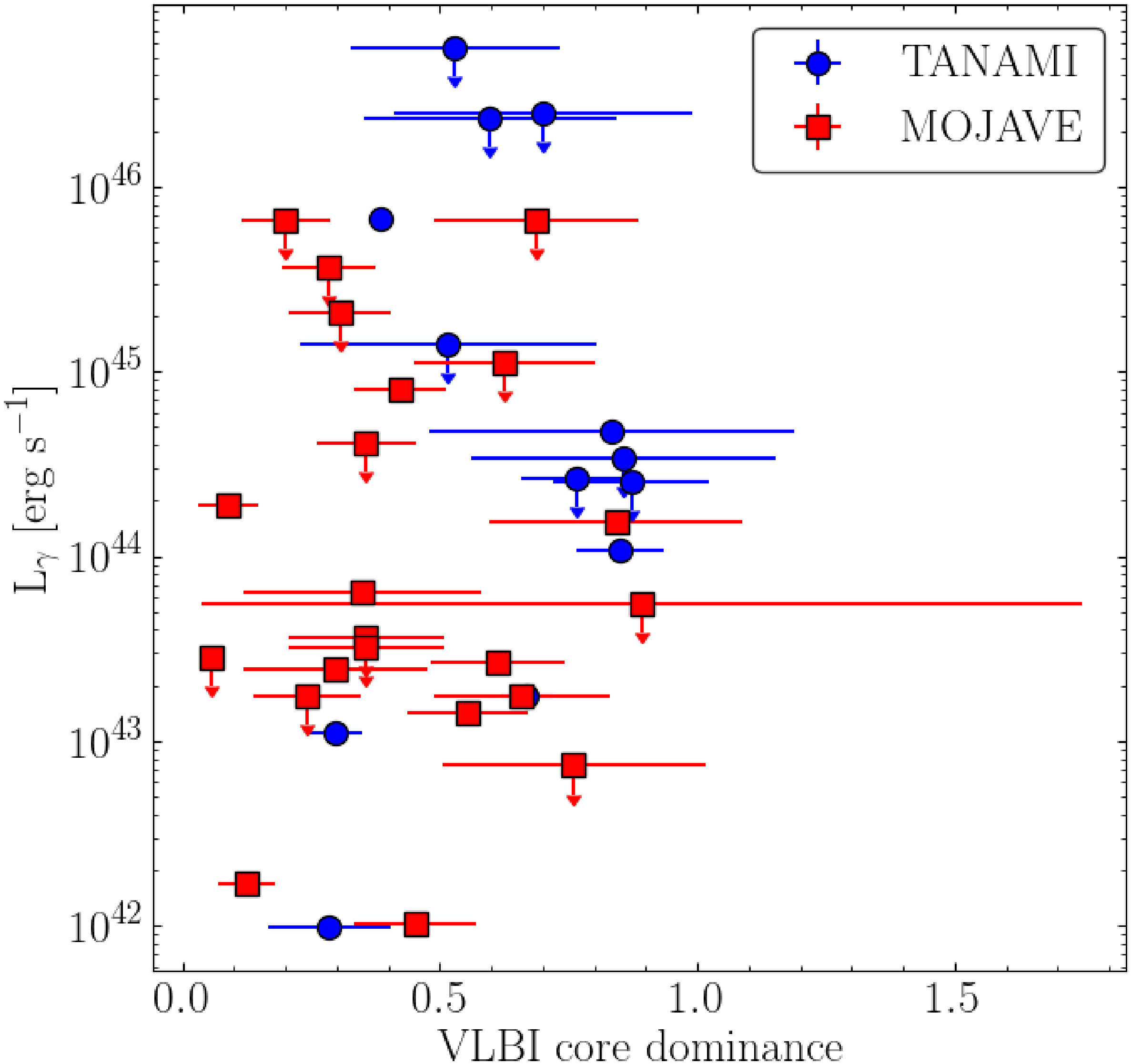

Kendall's tau

$\tau = 0.16$

p-value $= 0.17$

High-energy emission unrelated to Doppler boosting markers

VLBI core T_b vs. LAT luminosity

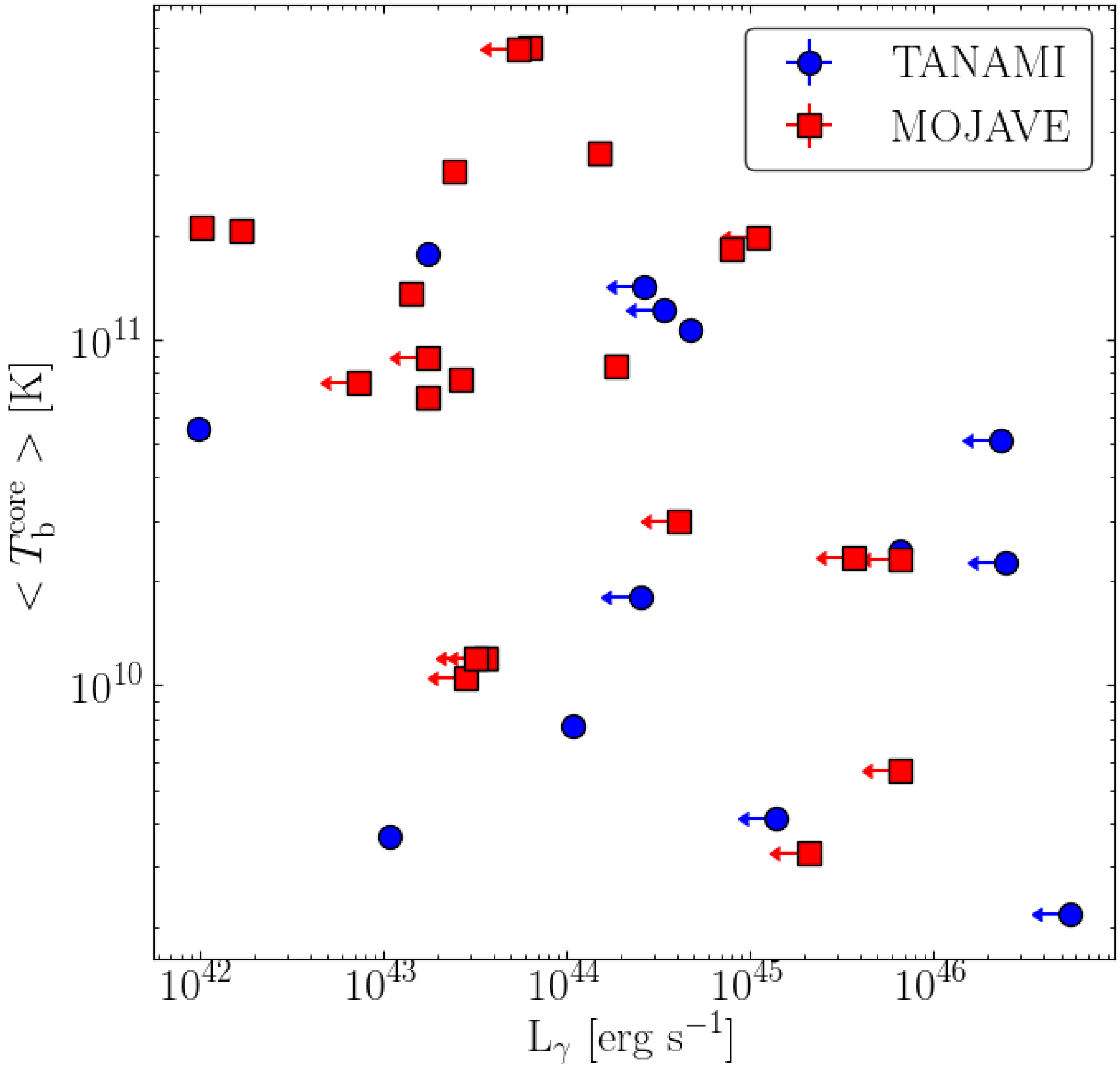

Kendall's tau
$\tau = 0.08$
p-value $= 0.5$

High-energy emission unrelated to Doppler boosting markers

Conclusions

- We have performed the first systematic study on the connection between pc-scale properties and high energy emission in misaligned jets

Conclusions

- We have performed the first systematic study on the connection between pc-scale properties and high energy emission in misaligned jets
- Selected individual source result: Pictor A
  - First counter-jet detection, improved intrinsic jet parameter estimates
  - Possible association between component ejection and gamma-ray activity

Conclusions

- We have performed the first systematic study on the connection between pc-scale properties and high energy emission in misaligned jets
- Selected individual source result: Pictor A
  - First counter-jet detection, improved intrinsic jet parameter estimates
  - Possible association between component ejection and gamma-ray activity
- Selected individual source result: PKS 0521−36
  - Subluminal apparent speed
  - Fast gamma-ray variability corresponds to core brightening but no jet morphological changes

Conclusions

- We have performed the first systematic study on the connection between pc-scale properties and high energy emission in misaligned jets
- Selected individual source result: Pictor A
  - First counter-jet detection, improved intrinsic jet parameter estimates
  - Possible association between component ejection and gamma-ray activity
- Selected individual source result: PKS 0521−36
  - Subluminal apparent speed
  - Fast gamma-ray variability corresponds to core brightening but no jet morphological changes
- **Gamma-ray emission in radio galaxies:**
  - **High-energy flux correlates with pc-scale radio core flux**
  - **No significant correlation with Doppler boosting markers**

Conclusions

- We have performed the first systematic study on the connection between pc-scale properties and high energy emission in misaligned jets
- Selected individual source result: Pictor A
  - First counter-jet detection, improved intrinsic jet parameter estimates
  - Possible association between component ejection and gamma-ray activity
- Selected individual source result: PKS 0521−36
  - Subluminal apparent speed
  - Fast gamma-ray variability corresponds to core brightening but no jet morphological changes
- **Gamma-ray emission in radio galaxies:**
  - **High-energy flux correlates with pc-scale radio core flux**
  - **No significant correlation with Doppler boosting markers**

Thank you for the attention!